Journal of Statistical Physics, Vol. 40, Nos. 3/4, 1985

Fluctuations in a Fluid Under a Stationary Heat Flux II. Slow Part of the Correlation Matrix

R. Schmitz[1] and E. G. D. Cohen[2]

Received January 22, 1985

The general formulas, derived in a previous paper, are used to calculate the correlation functions of the hydrodynamic variables in the Rayleigh–Bénard system. The behavior of the correlation functions on a time scale slow compared to that of sound propagation is determined, using systematically nonequilibrium hydrodynamic eigenmodes. These (slow) eigenmodes of the linearized Boussinesq equations in the presence of gravity and a temperature gradient are the viscous and the visco-heat modes. They are determined for ideal heat-conducting plates with stick boundary conditions. The visco-heat modes are found to behave qualitatively different from those obtained with slip boundary conditions. Using these eigenmodes, the slow part of the correlation functions can be determined explicitly. On a small length scale, as probed by light scattering, we recover the same expression for the Rayleigh line as quoted in the literature. On larger length scales, as probed by microwaves, the coupling of gravity to the temperature gradient gives rise to a convective instability (heating form below) or to propagating visco-heat modes (heating from above). The corresponding correlation functions and the Rayleigh line are calculated and discussed.

KEY WORDS: Rayleigh–Bénard system; fluctuations; correlation functions; viscous mode; visco-heat modes; Rayleigh number; convective instability; propagating modes; light scattering; microwave scattering; Rayleigh line.

1. INTRODUCTION

In a preceding paper[1] (hereafter referred to as I) we have derived the basic formulas for a unified treatment of the correlation functions of the hydrodynamic variables in a Rayleigh–Bénard system, i.e., a fluid between

[1] Institut für Theoretische Physik A, R. W. T. H. Aachen, Templergraben 55, D-5100 Aachen, Federal Republic of Germany.

[2] The Rockefeller University, 1230 York Avenue, New York, New York 10021.

0022-4715/85/0800-0431$04.50/0

two horizontal plates which is exposed to a stationary heat flux in the presence of a gravity field. We have shown that in the nonequilibrium stationary state the hydrodynamic fluctuations evolve on a slow and a fast time scale that are widely separated. In this paper we will investigate in more detail the fluctuations on the slow time scale. We will discuss in particular the slow part of the hydrodynamic correlation matrix which follows from the full hydrodynamic correlation matrix by averaging over times that are large on the fast time scale, but small on the slow time scale. As we have pointed out in I, Section 8, it is only the slow nonequilibrium hydrodynamic modes, i.e., the viscous and the visco-heat modes, that contribute to the slow part of the correlation matrix; the contribution from the fast hydrodynamic modes, i.e., the sound modes, average to zero on the slow time scale.

Our results for the slow part of the correlation matrix allow us to treat the following two problems as special applications: the Rayleigh line in a light-scattering experiment and the singular behavior of the correlation functions near the convective instability.

In a light-scattering experiment one measures in principle the Fourier transform of the density–density correlation function.[2] The light-scattering spectrum consists of three, well-separated lines: a Rayleigh line and two Brillouin lines. It is only the Rayleigh line that is generated by the slow part of the density–density correlation function. The Rayleigh line has a Lorentzian shape when the fluid is in thermal equilibrium.[3]

For a fluid exposed to a stationary heat flux Ronis *et al.*[4] and Kirkpatrick *et al.*[5] have shown that to first order in the temperature gradient the Rayleigh line is unaffected. Kirkpatrick, one of us (E.G.D.C.), and Dorfman[6] have also computed the Rayleigh line for large temperature gradients applying kinetic theory, as well as mode-coupling theory. In addition to an equilibriumlike Lorentzian part it has been found that there is also a non-Lorentzian contribution to the line, owing to mode-coupling effects, which is of second order in the temperature gradient. The total intensity of the Rayleigh line has a part that is inversely proportional to the fourth power of the wave vector. This behavior implies long-range density–density correlations at equal times in real space that are absent in equilibrium. For a special scattering geometry, Ronis and Procaccia[7] have confirmed these results by using fluctuating hydrodynamics. The equivalence of the kinetic, the mode-coupling, and the fluctuating hydrodynamics approach has been shown in I. Since the spatial distances probed in a normal light-scattering experiment are small one can neglect the gravity field and boundary effects, as has been done in Refs. 6 and 7.

Gravity does play an important role near the convective instability, however. In fact, for a fluid heated from below, it is the coupling of the

temperature gradient and the buoyancy force that causes the convective instability.[8] The onset of the instability and the quantitative details of the correlation functions near the instability depend much on the boundary conditions employed on the horizontal plates. Without specifying the boundary conditions, Zaĭtsev and Shliomis[9] have been able to describe the singular behavior of the temperature–temperature correlation function near the instability qualitatively from fluctuating hydrodynamics. More explicit results for the density–density correlation function near the instability have been obtained by Kirkpatrick and one of us (E.G.D.C.)[10] in the framework of kinetic theory. In that work it was assumed that the plates are ideal heat-conducting and—for the sake of mathematical simplicity—that the fluid obeys slip boundary conditions on the plates.

In this paper we include the gravity field systematically in the computation of the correlation matrix, and we use the physically more realistic, though mathematically more complicated, stick boundary conditions. Whether gravity can be neglected or not turns out to depend on the distance between the two points in which the correlation functions are computed. We show that there is a certain characteristic length below which gravity is negligible and rederive in this way the result for the Rayleigh line reported before.[6,7] For distances larger than the characteristic length, however, gravity must be taken into account, regardless of whether one is close to the instability or not.

The coupling of the gravity field to the temperature gradient can not only cause the convective instability, but, in the case the fluid is heated from above, also the propagation of some of the visco-heat modes.[8] If a light-scattering experiment were performed to measure these effects on the correlation functions, the wave vector would have to be small enough to probe the large length scale involved. For an incident laser beam with a wavelength in the regime of normal light this would require an extremely small scattering angle.[2] A way to avoid this experimental difficulty could be the reduction of the frequency of the incident beam by scattering microwaves. In spite of the technical problems to overcome in microwave scattering, we do compute the Rayleigh line for these very small wave vectors numerically for a few examples, taking also into account explicitly the boundary conditions.

Our calculation of the slow part of the correlation matrix is based on the explicit solution of the eigenvalue problems for the slow nonequilibrium hydrodynamic modes, which are the eigenmodes of the linearized Boussinesq equations,[1] for ideal heat-conducting plates with stick boundary conditions. While the viscous modes are trivial to compute and do not crucially depend on the boundary conditions we find that the behavior of the eigenvalues of the visco-heat modes, considered as functions of the tem-

perature gradient, are qualitatively different from the results obtained by employing slip boundary conditions. A few graphs will illustrate the more complicated behavior.

The plan of II is as follows: In Section 2 we summarize the basic equations derived in I, as they are relevant for the computation of the slow part of the correlation matrix. Then, in Section 3, we evaluate the slow part of the correlation matrix for points which are far away from the boundaries, so that boundary conditions can be neglected. In particular, we compute explicitly the long-range mode-coupling contribution to the equal-time correlation matrix for distances in the regime probed in normal light-scattering experiments. In Section 4 we describe how the slow modes are computed for ideal heat-conducting plates with stick boundary conditions. In particular, the behavior of the visco-heat modes is then discussed in Section 5. In Section 6 we apply the methods developed in Section 4 to compute the asymptotic behavior of the correlation matrix near the convective instability in a mean field theory. Finally, we present in Section 7 the results for the dynamic structure factor for the Rayleigh line. We will end this paper with a discussion and four short Appendices which provide some auxiliary results used in the main text, and illustrate some more formal statements by examples.

In the following paper III we will compute the fast part of the correlation matrix and the Brillouin lines of the light-scattering spectrum, thus completing our treatment of the properties of a fluid under a stationary heat flux by means of nonequilibrium eigenmodes.

2. BASIC EQUATIONS

As in I we consider a simple fluid in a gravity field $\mathbf{g} = -g\mathbf{e}_z$ between two horizontal, infinite plates, located at $z = -d/2$ and $z = +d/2$, which have uniform temperatures T_1 and T_2, respectively. We assume that the fluid has reached a nonconvective stationary state. The macroscopic fields, i.e., the pressure p, the temperature T, and the flow velocity $\mathbf{u}$, follow then from the nonlinear equations

$$\frac{dp}{dz} + g\rho = 0 \tag{2.1a}$$

$$\frac{d}{dz}\lambda\frac{dT}{dz} = 0 \tag{2.1b}$$

$$\mathbf{u} = 0 \tag{2.1c}$$

with the boundary conditions $p(d/2) = p_2$, $T(-d/2) = T_1$ and $T(d/2) = T_2$, where p_2 is the outside pressure. In (2.1), $\rho = \rho(p, T)$ is the mass density and $\lambda = \lambda(p, T)$ is the thermal conductivity.

We want to study the thermal fluctuations

$$\delta \mathbf{a} = \begin{pmatrix} \delta p \\ \delta T \\ \delta \mathbf{u} \end{pmatrix} \tag{2.2}$$

around a given steady state solution $\mathbf{a} = (p, T, \mathbf{u})$ with $p = p(z)$, $T = T(z)$ and $\mathbf{u} = 0$. In particular, we are interested in the correlation matrix

$$\mathsf{M}(\mathbf{r}_1, t_1; \mathbf{r}_2, t_2) = \langle \delta \mathbf{a}(\mathbf{r}_1, t_1)\, \delta \mathbf{a}(\mathbf{r}_2, t_2) \rangle_{\mathrm{ss}} \tag{2.3}$$

where the average is taken over the nonequilibrium steady state. In I we have shown how $\mathsf{M}(\mathbf{r}_1, t_1; \mathbf{r}_2, t_2)$ can be computed from fluctuating hydrodynamics for all distances $|\mathbf{r}_1 - \mathbf{r}_2|$ and time intervals $|t_1 - t_2|$ of hydrodynamic order with the restriction that $|z_1 - z_2|$ does not exceed a length l_0 which is chosen such that the spatial variation of the average quantities can be neglected within a fluid layer of height l_0. This means that l_0 must be small on the macroscopic length scale $L_\nabla \simeq [(1/a)(da/dz)]^{-1}$ where $a(z) = a(p(z), T(z))$ stands for the average quantity which varies most with position.

We recall from I that the correlation matrix can be expressed in terms of the nonequilibrium hydrodynamic modes, i.e., the normal modes of the hydrodynamic operator which is obtained by linearizing the hydrodynamic equations around the steady state solution. From the properties of these modes follows that the behavior of $\mathsf{M}(\mathbf{r}_1, t_1; \mathbf{r}_2, t_2)$ as function of $t = t_1 - t_2$ can be described on two widely separated time scales. In this paper we will be concerned with a detailed discussion of the temporal behavior of the correlation matrix on the slow time scale. We will denote by $\mathsf{M}^{(\mathrm{sl})}(\mathbf{r}_1, t_1; \mathbf{r}_2, t_2)$ the slow part of $\mathsf{M}(\mathbf{r}_1, t_1; \mathbf{r}_2, t_2)$, i.e., the matrix obtained from M by averaging over times $t_1 - t_2$ which are large on the fast time scale, but small on the slow one. On the slow time scale the contributions from the fast hydrodynamic modes, i.e., the sound modes, to M are averaged to zero, so that only the slow modes, namely, the viscous and the visco-heat modes, contribute to $\mathsf{M}^{(\mathrm{sl})}$.

In (I.7.1)[3] we have derived the eigenvalue equations for the viscous

[3] Equation numbers preceded by "I" are those from paper I (Ref. 1).

modes (to be denoted by the index ν) for a given horizontal wavevector $\mathbf{k}_{\|}(k_x, k_y)$:

$$\nu\mathscr{D}\xi^R_{\nu,k_{\|}n}(z) = s_{\nu,k_{\|}n}\xi^R_{\nu,k_{\|}n}(z) \tag{2.4}$$

where ν is the kinematic viscosity [cf. (I.5.14)] and $\mathscr{D} = k_{\|}^2 - d^2/dz^2$. Furthermore n is a discrete index to count the different modes. The eigenvalues $s_{\nu,k_{\|}n}$ and right-eigenfunctions $\xi^R_{\nu,k_{\|}n}(z) = (\nabla \times \mathbf{u}^R_{\nu,k_{\|}n}) \cdot \mathbf{e}_z$ is the z component of the vorticity. The left-eigenfunction $\xi^L_{\nu,k_{\|}n}(z)$ obeys the same equation (2.4) and the normalization is given by Eq. (I.7.8a):

$$\int_{-d/2}^{d/2} \xi^{L*}_{\nu,k_{\|}n}\xi^R_{\nu,k_{\|}m}\, dz = \frac{k_{\|}^2}{(2\pi)^2}\delta_{nm} \tag{2.5}$$

The visco-heat modes (to be denoted by the index λ) obey the coupled eigenvalue equations (I.7.4):

$$\begin{pmatrix} D_T\mathscr{D} & \dfrac{dT}{dz} \\ -\alpha g k_{\|}^2 & \nu\mathscr{D}^2 \end{pmatrix} \begin{pmatrix} T^R_{\lambda,k_{\|}n}(z) \\ v^R_{\lambda,k_{\|}n}(z) \end{pmatrix} = s_{\lambda,k_{\|}n} \begin{pmatrix} T^R_{\lambda,k_{\|}n}(z) \\ \mathscr{D}v^R_{\lambda,k_{\|}n}(z) \end{pmatrix} \tag{2.6}$$

where α is the thermal expansion coefficient and D_T is the thermal diffusivity [cf. (I.5.14)]. The components of the right eigenvector $(T^R_{\lambda,k_{\|}n}, v^R_{\lambda,k_{\|}n})$ are the temperature and the z component of the transversal part of the flow velocity, respectively. The left eigenvectors $(T^L_{\lambda,k_{\|}n}, v^L_{\lambda,k_{\|}n})$ follow from the adjoint eigenvalue problem of (2.6) in the scalar product to be defined in (2.7) below. We derive the left eigenvalue equations in Appendix A. The normalization is [cf. (I.7.8b)]

$$\int_{-d/2}^{d/2} \left[v^{L*}_{\lambda,k_{\|}n} v^R_{\lambda,k_{\|}m} + \frac{1}{k_{\|}^2}\frac{dv^{L*}_{\lambda,k_{\|}n}}{dz}\frac{dv^R_{\lambda,k_{\|}m}}{dz} + T^{L*}_{\lambda,k_{\|}n} T^R_{\lambda,k_{\|}m} \right] dz = \frac{1}{(2\pi)^2}\delta_{nm} \tag{2.7}$$

In (2.4) and (2.6) the values of the steady state quantities α, dT/dz, ν, and D_T have to be taken in a reference point R_z on the z axis in the center of a fluid layer of height $l_0 \ll L_V$ to which z_1 and z_2 belong; their spatial variation can be neglected in this layer. The eigenvalue equations (2.4) and (2.6) to be solved in this paper, are equivalent to the linearized Boussinesq equations.[1,11]

Finally we will quote some basic formulas derived in I from which the slow part of the correlation matrix can be computed explicitly. Using (I.8.8) and that the contributions from the sound modes are averaged to zero on the slow time scale, we find that $\mathsf{M}^{(sl)}(\mathbf{r}_1, t_1; \mathbf{r}_2, t_2)$ can be expressed in terms of the following four scalar correlation functions:

$$
\begin{aligned}
S(r_\parallel, z_1, z_2; t) &= k_B \frac{c_p^2}{T^2} \cdot 2\pi \sum_n \int_0^\infty dk_\parallel \, k_\parallel J_0(k_\parallel r_\parallel) \\
&\quad \times e^{-s_{\lambda,k_\parallel n} t} T^R_{\lambda,k_\parallel n}(z_1) \, \theta_{\lambda,k_\parallel n}(z_2) \\
S'(r_\parallel, z_1, z_2; t) &= k_B \frac{c_p}{T} \cdot 2\pi \sum_n \int_0^\infty dk_\parallel \, k_\parallel J_0(k_\parallel r_\parallel) \\
&\quad \times \frac{e^{-s_{\lambda,k_\parallel n} t}}{k_\parallel^2} \, T^R_{\lambda,k_\parallel n}(z_1) \, w_{\lambda,k_\parallel n}(z_2) \\
V(r_\parallel, z_1, z_2; t) &= k_B \cdot 2\pi \sum_n \int_0^\infty dk_\parallel \, k_\parallel J_0(k_\parallel r_\parallel) \\
&\quad \times \frac{e^{-s_{\lambda,k_\parallel n} t}}{k_\parallel^4} \, v^R_{\lambda,k_\parallel n}(z_1) \, w_{\lambda,k_\parallel n}(z_2)
\end{aligned}
\tag{2.8a}
$$

and

$$
\begin{aligned}
\Xi(r_\parallel, z_1, z_2; t) &= k_B \frac{T}{\rho} \cdot 2\pi \sum_n \int_0^\infty dk_\parallel \, k_\parallel J_0(k_\parallel r_\parallel) \\
&\quad \times \frac{e^{-s_{\lambda,k_\parallel n} t}}{k_\parallel^4} \, \xi^R_{\lambda,k_\parallel n}(z_1) \, \xi^{L*}_{\nu,k_\parallel n}(z_2)
\end{aligned}
\tag{2.8b}
$$

Here $\mathbf{r}_\parallel = (x, y) = (x_1 - x_2, y_1 - y_2)$, $r_\parallel = |\mathbf{r}_\parallel|$, $t = t_1 - t_2 > 0$ and $J_0(x)$ is the Bessel function of order zero. Furthermore k_B is the Boltzmann constant and c_p is the specific heat at constant pressure per unit mass. We recall from I that $S(r_\parallel, z_1, z_2; t)$ is the entropy–entropy correlation function. In (2.8a) the functions $\theta_{\lambda,k_\parallel n}(z_2)$ and $w_{\lambda,k_\parallel n}(z_2)$ are defined as

$$
\begin{aligned}
\theta_{\lambda,k_\parallel n}(z_2) &= \frac{T^2}{\rho c_p} T^{L*}_{\lambda,k_\parallel n}(z_2) - (2\pi)^2 \sum_m \frac{\Lambda_{nm}}{s_{\lambda,k_\parallel n} + s_{\lambda,k_\parallel m}} T^R_{\lambda,k_\parallel m}(z_2) \\
w_{\lambda,k_\parallel n}(z_2) &= \frac{T}{\rho} v^{L*}_{\lambda,k_\parallel n}(z_2) - (2\pi)^2 \sum_m \frac{\Lambda_{nm}}{s_{\lambda,k_\parallel n} + s_{\lambda,k_\parallel m}} v^R_{\lambda,k_\parallel m}(z_2)
\end{aligned}
\tag{2.9}
$$

They consist of a local equilibrium part [first term on the right-hand side (r.h.s.) of (2.9)] and a mode-coupling part [second term on the r.h.s. of (2.9)], which vanishes in equilibrium and gives rise to long-range correlations at equal times, i.e., for $t = 0$. The mode-coupling coefficients Λ_{nm} in (2.9) are defined as

$$
\Lambda_{nm} = \int_{-d/2}^{d/2} \frac{T}{\rho} \frac{dT}{dz} \left[T^{L*}_{\lambda,k_\parallel n} v^{L*}_{\lambda,k_\parallel m} + v^{L*}_{\lambda,k_\parallel n} T^{L*}_{\lambda,k_\parallel m} \right] dz \tag{2.10}
$$

Using (I.2.9), (I.2.10) and (I.8.9) the components of $\mathsf{M}^{(\mathrm{sl})}(\mathbf{r}_1, t_1; \mathbf{r}_2, t_2)$ for times $t = t_1 - t_2 > 0$ are:

$$\begin{aligned} M_{pp}^{(\mathrm{sl})} &= 0, \qquad M_{pT}^{(\mathrm{sl})} = 0, \qquad M_{TT}^{(\mathrm{sl})} = g_{TT}^{(\mathrm{sl})} \\ \mathbf{M}_{p\mathbf{u}}^{(\mathrm{sl})} &= 0, \qquad \mathbf{M}_{T\mathbf{u}}^{(\mathrm{sl})} = f_{T1}^{(\mathrm{sl})}\mathbf{e}_z + f_{T2}^{(\mathrm{sl})}\hat{\mathbf{r}}_{\|} \\ \mathsf{M}_{\mathbf{uu}}^{(\mathrm{sl})} &= h_1^{(\mathrm{sl})}(1 - \mathbf{e}_z\mathbf{e}_z) + h_2^{(\mathrm{sl})}\mathbf{e}_z\mathbf{e}_z + h_3^{(\mathrm{sl})}\hat{\mathbf{r}}_{\|}\hat{\mathbf{r}}_{\|} \\ &\quad + h_4^{(\mathrm{sl})}\mathbf{e}_z\hat{\mathbf{r}}_{\|} + h_5^{(\mathrm{sl})}\hat{\mathbf{r}}_{\|}\mathbf{e}_z \end{aligned} \tag{2.11}$$

where $\hat{\mathbf{r}}_{\|} = \mathbf{r}_{\|}/r_{\|}$ and

$$g_{TT}^{(\mathrm{sl})} = \frac{T^2}{c_p^2} S$$

$$f_{T1}^{(\mathrm{sl})} = -\frac{T}{c_p}\left(\frac{\partial}{\partial r_{\|}} + \frac{1}{r_{\|}}\right)\frac{\partial S'}{\partial r_{\|}}, \qquad f_{T2}^{(\mathrm{sl})} = -\frac{T}{c_p}\frac{\partial}{\partial z_2}\frac{\partial S'}{\partial r_{\|}}$$

$$h_1^{(\mathrm{sl})} = -\frac{\partial^2 \Xi}{\partial r_{\|}^2} - \frac{1}{r_{\|}}\frac{\partial}{\partial r_{\|}}\frac{\partial^2 V}{\partial z_1\, \partial z_2}, \qquad h_2^{(\mathrm{sl})} = \left[\left(\frac{\partial}{\partial r_{\|}} + \frac{1}{r_{\|}}\right)\frac{\partial}{\partial r_{\|}}\right]^2 V$$

$$h_3^{(\mathrm{sl})} = -\left(\frac{\partial}{\partial r_{\|}} - \frac{1}{r_{\|}}\right)\frac{\partial}{\partial r_{\|}}\left[-\Xi + \frac{\partial^2 V}{\partial z_1\, \partial z_2}\right]$$

$$h_4^{(\mathrm{sl})} = \frac{\partial}{\partial r_{\|}}\left(\frac{\partial}{\partial r_{\|}} + \frac{1}{r_{\|}}\right)\frac{\partial}{\partial r_{\|}}\frac{\partial V}{\partial z_2}$$

$$h_5^{(\mathrm{sl})}(r_{\|}, z_1, z_2; t) = -h_4^{(\mathrm{sl})}(r_{\|}, z_2, z_1; -t) \tag{2.12}$$

In (2.8), (2.9), and (2.12) the values of the steady state quantities must be taken in the reference point R_z. For the off-diagonal elements, not quoted in (2.11), and for times $t < 0$ one can use the symmetry relation

$$\mathsf{M}^{(\mathrm{sl})}(\mathbf{r}_2, t_2; \mathbf{r}_1, t_1) = \mathsf{M}^{(\mathrm{sl})^T}(\mathbf{r}_1, t_1; \mathbf{r}_2, t_2) \tag{2.13}$$

where the superscript T denotes the transposed matrix.

Equations (2.4)–(2.13) are a self-contained set of equations for the slow part of the correlation matrix on which our further considerations will be based.

3. CORRELATIONS IN THE BULK FLUID

As a first application we compute in this section $\mathsf{M}^{(\mathrm{sl})}(\mathbf{r}_1, t_1; \mathbf{r}_2, t_2)$ for points $\mathbf{r}_1$, $\mathbf{r}_2$, the z coordinates of which not only obey the condition $|z_1 - z_2| \leqslant l_0 \ll L_\nabla$, but which also stay away from the boundaries, i.e.,

$|z_1 - z_2| \ll d$ and $|z_1 + z_2| \ll d$. In this case we may treat the system as infinite also in the z direction. As reference point we choose the center of mass $R_z = \frac{1}{2}(z_1 + z_2)$ and take the values of all the steady state quantities in the point R_z.

To calculate $\mathsf{M}^{(\mathrm{sl})}$ we have therefore first to solve the eigenvalue equations (2.4)–(2.7) for a system that is infinite in the z direction. With the aid of these modes we will then compute the four scalar functions S, S', V, and Ξ, defined in (2.8)–(2.10). They determine the slow part of the correlation matrix, according to (2.11)–(2.13).

For an infinite system the eigenfunctions are proportional to plane waves $e^{ik_z z}$, where k_z can be any real wave number. The eigenvalues of the viscous modes [Eq. (2.4)] are

$$S_{\nu, k_\parallel k_z} = \nu k^2 \tag{3.1}$$

where we have set

$$k^2 = k_\parallel^2 + k_z^2 \tag{3.2}$$

Using (2.5) the normalized right and left eigenfunctions are

$$\xi^R_{\nu, k_\parallel k_z}(z) = \xi^L_{\nu, k_\parallel k_z}(z) = \frac{k_\parallel}{(2\pi)^{3/2}} e^{ik_z z} \tag{3.3}$$

Inserting (3.1) and (3.3) into (2.8b) yields

$$\Xi(r_\parallel, z_1, z_2; t) = k_B \frac{T}{\rho} \frac{1}{(2\pi)^2} \int_{-\infty}^{\infty} dk_z \int_0^{\infty} dk_\parallel \, k_\parallel J_0(k_\parallel r_\parallel) \times e^{ik_z(z_1 - z_2)} \frac{e^{-\nu k^2 t}}{k_\parallel^2} \tag{3.4}$$

The eigenvalues of the visco-heat modes [Eq. (2.6)] are

$$s_{\lambda_\pm, k_\parallel k_z} = \frac{\nu + D_T}{2} k^2 \pm \frac{\nu - D_T}{2} k^2 \left[1 - \frac{4\alpha g}{(\nu - D_T)^2} \frac{dT}{dz} \frac{k_\parallel^2}{k^6} \right]^{1/2} \tag{3.5}$$

The right eigenvectors follow from (2.6), while the left eigenvectors are obtained from Eq. (A.13) of Appendix A. Normalizing according to (2.7) the right and left eigenvectors are

$$\begin{aligned} T^R_{\lambda_\pm, k_\parallel k_z}(z) &= \pm \frac{k_\parallel}{(2\pi)^{3/2}} \frac{dT}{dz} \frac{1}{k^2} e^{ik_z z} \\ v^R_{\lambda_\pm, k_\parallel k_z}(z) &= \pm \frac{k_\parallel}{(2\pi)^{3/2}} \frac{s_{\lambda_\pm, k_\parallel k_z} - D_T k^2}{k^2} e^{ik_z z} \end{aligned} \tag{3.6}$$

and

$$T^L_{\lambda_\pm,k_\parallel k_z}(z) = -\frac{k_\parallel}{(2\pi)^{3/2}} \frac{\alpha g}{s^*_{\lambda_+,k_\parallel k_z} - s^*_{\lambda_-,k_\parallel k_z}} \frac{1}{s^*_{\lambda_\pm,k_\parallel k_z} - D_T k^2} e^{ik_z z}$$

$$v^L_{\lambda_\pm,k_\parallel k_z}(z) = \frac{k_\parallel}{(2\pi)^{3/2}} \frac{1}{s^*_{\lambda_+,k_\parallel k_z} - s^*_{\lambda_-,k_\parallel k_z}} e^{ik_z z} \tag{3.7}$$

respectively.

Using the left eigenvectors we can easily calculate the mode-coupling coefficients $\Lambda_{k_z\lambda_\pm,k'_z\lambda'_\mp}$ from (2.10) where, for consistency, the bounds of integration must be extended to infinity, and the value of $(T/\rho)(dT/dz)$ is taken in the reference point R_z. After computing the functions $\theta_{\lambda_\pm,k_\parallel k_z}(z_2)$ and $w_{\lambda_\pm,k_\parallel k_z}(z_2)$ with the aid of (2.9), we find from (2.8a) for the entropy–entropy correlation function

$$\begin{aligned} S(r_\parallel, z_1, z_2; t) &= k_B \frac{c_p^2}{\rho T} \frac{1}{(2\pi)^2} \int_{-\infty}^{\infty} dk_z \int_0^{\infty} dk_\parallel\, k_\parallel J_0(k_\parallel r_\parallel)\, e^{ik_z(z_1 - z_2)} \\ &\quad \times \frac{1}{s_+ - s_-} \left\{ \frac{T}{c_p} \left[(s_+ - \nu k^2)\, e^{-s_+ t} + (\nu k^2 - s_-)\, e^{-s_- t} \right] \right. \\ &\quad \left. - \left(\frac{dT}{dz}\right)^2 \frac{\nu}{\nu + D_T} \frac{k_\parallel^2}{k^2} \left(\frac{e^{-s_+ t}}{s_+} - \frac{e^{-s_- t}}{s_-} \right) \right\} \end{aligned} \tag{3.8}$$

where we have written $s_\pm$ as abbreviation for the eigenvalues $s_{\lambda_\pm,k_\parallel k_z}$. The two terms in the curly brackets correspond to the local equilibrium part and the mode-coupling part, respectively. Similarly we find

$$\begin{aligned} S'(r_\parallel, z_1, z_2; t) &= k_B \frac{c_p}{\rho} \frac{dT}{dz} \frac{1}{(2\pi)^2} \int_{-\infty}^{\infty} dk_z \int_0^{\infty} dk_\parallel\, k_\parallel J_0(k_\parallel r_\parallel) \\ &\quad \times e^{ik_z(z_1 - z_2)} \frac{1}{(s_+ - s_-)\, k^2} \left\{ (e^{-s_+ t} - e^{-s_- t}) \right. \\ &\quad \left. - \frac{D_T}{\nu + D_T} \left(\frac{s_+ - \nu k^2}{s_+} e^{-s_+ t} + \frac{\nu k^2 - s_-}{s_-} e^{-s_- t} \right) \right\} \end{aligned} \tag{3.9}$$

This quantity vanishes in equilibrium.

Finally

$$V(r_{\|}, z_1, z_2; t) = k_B \frac{T}{\rho} \frac{1}{(2\pi)^2} \int_{-\infty}^{\infty} dk_z \int_0^{\infty} dk_{\|}\, k_{\|} J_0(k_{\|} r_{\|}) \times e^{ik_z(z_1 - z_2)} \frac{1}{(s_+ - s_-)\, k^2 k_{\|}^2} \times \left\{ [(s_+ - D_T k^2)\, e^{-s_+ t} + (D_T k^2 - s_-)\, e^{-s_- t}] + \alpha g \frac{dT}{dz} \frac{D_T}{\nu + D_T} \frac{k_{\|}^2}{k^2} \left(\frac{e^{-s_+ t}}{s_+} - \frac{e^{-s_- t}}{s_-} \right) \right\} \tag{3.10}$$

We remark that the correlation functions (3.4) and (3.8)–(3.10) depend on z_1 and z_2 only via $|z_1 - z_2|$.[4] Carrying out the necessary differentiations, $\mathsf{M}^{(\mathrm{sl})}(\mathbf{r}_1, t_1; \mathbf{r}_2, t_2)$ can now be determined with Eqs. (2.11) and (2.12). We will not write down the explicit expressions for $\mathsf{M}^{(\mathrm{sl})}$ here, since they are rather lengthy. Instead we restrict ourselves now to small distances that are probed in normal light-scattering experiments; more precisely we assume that $|\mathbf{r}_1 - \mathbf{r}_2|$ is much smaller than the characteristic length λ defined by

$$\lambda = \left| \frac{\alpha g}{\nu D_T} \frac{dT}{dz} \right|^{-1/4} \tag{3.11}$$

(see footnote 5). In this case $\mathsf{M}^{(\mathrm{sl})}(\mathbf{r}_1, t_1; \mathbf{r}_2, t_2)$ simplifies and we will give the expressions for the nonequilibrium part $\mathsf{D}^{(\mathrm{sl})}(\mathbf{r}_1, \mathbf{r}_2)$ of the equal-time correlation matrix $\mathsf{M}^{(\mathrm{sl})}(\mathbf{r}_1, t_2; \mathbf{r}_2, t_2)$ to expose explicitly the long-range behavior associated with the mode-coupling contributions.

For $|\mathbf{r}_1 - \mathbf{r}_2| \ll \lambda$ only the large wave vectors with $k \gg \lambda^{-1}$ contribute

[4] This implies that the slow part of the correlation matrix obeys the time-reversal symmetry $\mathsf{M}^{(\mathrm{sl})}(\mathbf{r}_1, t_1; \mathbf{r}_2, t_2) = \mathsf{M}^{(\mathrm{sl})}(\mathbf{r}_2, t_1; \mathbf{r}_1, t_2) = \mathsf{M}^{(\mathrm{sl})\dagger}(\mathbf{r}_1, t_2; \mathbf{r}_2, t_1)$ in the bulk fluid. In equilibrium, time-several symmetry holds even for the whole correlation matrix $\mathsf{M}(\mathbf{r}_1, t_1; \mathbf{r}_2, t_2)$. As we will see in paper III it is violated for the fast part of M in the nonequilibrium steady state. Notice that time-reversal symmetry is always violated when boundary conditions are included since M depends then on z_1 and z_2 separately.

[5] Of course, d should be much larger than λ, so that the infinite system approximation, made in this section, is justified. To give an idea of the magnitudes involved, we note that for water under normal conditions[12] and a temperature gradient of $dT/dz = 50\ \mathrm{K\ cm^{-1}}$ the characteristic length is $\lambda \approx 0.03$ cm, while typically $d \approx 0.1$ cm.

significantly to the Fourier integrals in (3.8)–(3.10). In this regime the eigenvalues (3.5) can be approximated by their equilibrium values

$$\begin{aligned} s_+ &\equiv s_{\lambda_+, k_\parallel k_z} \approx \nu k^2 \\ s_- &\equiv s_{\lambda_-, k_\parallel k_z} \approx D_T k^2 \end{aligned} \qquad (k \gg \lambda^{-1}) \tag{3.12}$$

Inserting (3.12) into (3.8)–(3.10), setting $t=0$, and carrying out the integrations we obtain

$$\begin{aligned} S(r_\parallel, z_1, z_2; 0) &= k_B \frac{c_p}{\rho} \delta(\mathbf{r}_1 - \mathbf{r}_2) \\ &\quad - k_B \frac{c_p^2}{\rho T} \left(\frac{dT}{dz}\right)^2 \frac{1}{D_T(\nu + D_T)} \frac{1}{32\pi} \left[3 - \frac{(z_1 - z_2)^2}{r^2}\right] r \\ S'(r_\parallel, z_1, z_2; 0) &= k_B \frac{c_p}{\rho} \frac{dT}{dz} \frac{1}{\nu + D_T} \frac{1}{8\pi} r \qquad (3.13a) \\ V(r_\parallel, z_1, z_2; 0) &= k_B \frac{T}{\rho} \frac{1}{(2\pi)^3} \int d\mathbf{k}\, e^{i\mathbf{k}\cdot(\mathbf{r}_1 - \mathbf{r}_2)} \frac{1}{k^2 k_\parallel^2} \\ &\quad + k_B \frac{T}{\rho} \alpha g \frac{dT}{dz} \frac{1}{\nu(\nu + D_T)} \frac{1}{2880\pi} r^5 \end{aligned}$$

Furthermore, from (3.4) we get

$$\Xi(r_\parallel, z_1, z_2; 0) = k_B \frac{T}{\rho} \frac{1}{(2\pi)^3} \int d\mathbf{k}\, e^{i\mathbf{k}\cdot(\mathbf{r}_1 - \mathbf{r}_2)} \frac{1}{k_\parallel^2} \tag{3.13b}$$

In (3.13) we have used $r = |\mathbf{r}_1 - \mathbf{r}_2| = [r_\parallel^2 + (z_1 - z_2)^2]^{1/2}$.

The mode-coupling contributions in (3.13) are those terms which are proportional to $1/(\nu + D_T)$. They increase with distance r by simple power laws and vanish, of course, in thermal equilibrium, i.e., for $dT/dz = 0$. The other terms in (3.13) are the local equilibrium contributions. It has been shown in I that the local equilibrium part $\mathsf{A}(\mathbf{r}_1, \mathbf{r}_2) = \mathsf{M}^{\text{L.E.}}(\mathbf{r}_1, t_2; \mathbf{r}_2, t_2)$ of the full equal-time correlation matrix is short-range, i.e., proportional to $\delta(\mathbf{r}_1 - \mathbf{r}_2)$. Nevertheless the local equilibrium parts of V and Ξ, represented in (3.13) by Fourier integrals, cause long-range parts in the velocity–velocity correlation function $\mathsf{A}_{\mathbf{uu}}(\mathbf{r}_1, \mathbf{r}_2) = \mathsf{M}_{\mathbf{uu}}^{\text{L.E.}}(\mathbf{r}_1, t_2; \mathbf{r}_2, t_2)$ when (3.13) is inserted into (2.11), (2.12). They arise because we have simply extrapolated our expressions for the slow part of the unequal-time correlation matrix for times $t_1 > t_2$ back towards equal times $t_1 = t_2$, thereby ignoring effects on the fast time scale, i.e., the sound modes. This extrapolation causes an "initial slip" effect,[13] i.e., a deviation of the

extrapolated initial value at $t_1 = t_2$ from the true one. When also the contributions from the sound modes, to be evaluated in III, are added these long-range contributions to $\mathsf{A}_{\mathbf{uu}}$ all cancel, and one obtains $\mathsf{A}_{\mathbf{uu}}(\mathbf{r}_1, \mathbf{r}_2) = k_B(T/\rho)\mathsf{1}\,\delta(\mathbf{r}_1 - \mathbf{r}_2)$, as it should be.

Computing finally the mode-coupling part $\mathsf{D}^{(\mathrm{sl})}(\mathbf{r}_1, \mathbf{r}_2)$ of the equal-time correlation matrix, we use (2.11), (2.12), (3.13), and that

$$h_j^{(\mathrm{sl})(\mathrm{M.C.})}(r_{\|}, z_1, z_2; 0) = k_B \frac{T}{\rho} \alpha g \frac{dT}{dz} \frac{1}{\nu(\nu + D_T)} \frac{1}{192\pi} l_j(z_1 - z_2, r) \qquad (j = 1,\ldots, 4) \tag{3.14}$$

where

$$\begin{aligned} l_1(z, r) &= \left(1 + \frac{z^2}{r^2}\right) r, & l_2(z, r) &= \left(15 - 6\frac{z^2}{r^2} - \frac{z^4}{r^4}\right) r \\ l_3(z, r) &= \left(1 - 2\frac{z^2}{r^2} + \frac{z^4}{r^4}\right) r, & l_4(z, r) &= \frac{z(r^2 - z^2)^{1/2}}{r^2}\left(3 + \frac{z^2}{r^2}\right) r \end{aligned} \tag{3.15}$$

to find explicitly for the nonvanishing elements of $\mathsf{D}^{(\mathrm{sl})}$:

$$D_{TT}^{(\mathrm{sl})}(\mathbf{r}_1, \mathbf{r}_2) = -k_B \frac{T}{\rho}\left(\frac{dT}{dz}\right)^2 \frac{1}{D_T(\nu + D_T)} \frac{1}{32\pi}\left(3 - \frac{z^2}{r^2}\right) r \tag{3.16a}$$

$$\mathbf{D}_{T\mathbf{u}}^{(\mathrm{sl})}(\mathbf{r}_1, \mathbf{r}_2) = -k_B \frac{T}{\rho} \frac{dT}{dz} \frac{1}{\nu + D_T} \frac{1}{8\pi}\left(\mathbf{e}_z + \frac{z}{r}\hat{\mathbf{r}}\right) \frac{1}{r} \tag{3.16b}$$

$$\mathsf{D}_{\mathbf{uu}}^{(\mathrm{sl})}(\mathbf{r}_1, \mathbf{r}_2) = k_B \frac{T}{\rho} \alpha g \frac{dT}{dz} \frac{1}{\nu(\nu + D_T)} \frac{1}{192\pi}\left[\left(1 + \frac{z^2}{r^2}\right)\mathsf{1} + 14\mathbf{e}_z\mathbf{e}_z + \left(1 - \frac{z^2}{r^2}\right)\hat{\mathbf{r}}\hat{\mathbf{r}} - 4\frac{z}{r}(\mathbf{e}_z\hat{\mathbf{r}} + \hat{\mathbf{r}}\mathbf{e}_z)\right] r \tag{3.16c}$$

where $\mathbf{r} = \mathbf{r}_1 - \mathbf{r}_2$, $\hat{\mathbf{r}} = \mathbf{r}/r$, and the values of the steady state quantities must be taken in the reference point $R_z = (1/2)(z_1 + z_2)$ on the z axis. The correlation functions $D_{TT}^{(\mathrm{sl})}$ and $D_{T\mathbf{u}}^{(\mathrm{sl})}$ are independent of the gravity field and of, respectively, second and first order in the temperature gradient. $\mathsf{D}_{\mathbf{uu}}^{(\mathrm{sl})}$ is proportional to the product $g(dT/dz)$. $D_{TT}^{(\mathrm{sl})}$ and $\mathsf{D}_{\mathbf{uu}}^{(\mathrm{sl})}$ increase linearly with the distance r, while $\mathbf{D}_{T\mathbf{u}}^{(\mathrm{sl})}$ decreases like r^{-1} in the regime considered here, i.e., $|\mathbf{r}_1 - \mathbf{r}_2| \ll \lambda$. The result for $D_{TT}^{(\mathrm{sl})}$ agrees with the expression in Ref. 6.

4. EIGENMODES FOR STICK BOUNDARY CONDITIONS

Boundary effects may no longer be neglected when the correlation matrix $\mathsf{M}^{(sl)}(\mathbf{r}_1, t_1; \mathbf{r}_2, t_2)$ is to be computed for the cases that one of the points $\mathbf{r}_1$, $\mathbf{r}_2$ lies close to a boundary or that the distance $|z_1 - z_2|$ approaches the size of the system d. Fluctuations on the length scale $|z_1 - z_2| \simeq d$ are particularly important near the convective instability since they become singular there.[9] But, as we will see in the subsequent sections, there are also interesting phenomena on that scale away from the instability.

We will restrict ourselves here to systems for which $d \approx l_0 \ll L_\nabla$.[6] Then we can take the values of all the steady state quantities at the reference point $R_z = 0$ and neglect their spatial variation throughout the system.

Usually it is assumed that the plates are ideal heat conductors and—for the sake of mathematical simplicity—that the fluid velocity obeys slip boundary conditions, i.e., the tangential components of the force density exerted by the plates on the fluid is zero. For these boundary conditions the slow part of the correlation matrix in a non-convective stationary state—near or away from the instability—is easily obtained from the results (3.4) and (3.8)–(3.10) when the domain of the continuous wave number k_z is restricted to the discrete values $k_z = n(\pi/d)$ $(n = 1, 2, 3, ...)$ and $(1/2\pi)\int_{-\infty}^{\infty} dk_z \exp[ik_z(z_1 - z_2)] \cdots$ is replaced by $(1/d)\sum_{n=1}^{\infty} \{\cos k_n(z_1 - z_2) \pm (-1)^n \cos[k_n(z_1 + z_2)]\} \cdots$. [The + sign must be used in (3.4), while in (3.8)–(3.10) the − sign is correct.] T. R. Kirkpatrick and one of us (E.G.D.C.) have computed the density–density and the velocity–velocity correlation functions for slip boundary conditions.[10]

We will concentrate in the following on the more realistic—but also more complicated—stick boundary conditions which require that the flow velocity on the plates be zero. We first consider the viscous modes, which are easy to determine. The right and the left modes both obey the second order differential equation (2.4). The stick boundary conditions are

$$\xi^R_{\nu,k_\parallel n} = 0 \qquad (z = \pm d/2) \tag{4.1}$$

and identical conditions hold for $\xi^L_{\nu,k_\parallel n}$. The eigenvalues are therefore

$$s_{\nu,k_\parallel n} = \nu(k_\parallel^2 + k_n^2) \qquad (n = 1, 2, ,...) \tag{4.2}$$

where we have set

$$k_n = n\frac{\pi}{d} \tag{4.3}$$

[6] This condition is realized in a Rayleigh–Bénard cell which typically has a size of $d = 0.1$ cm, while $L_\nabla \approx 6$ cm for water at $T = 300$ K and $dT/dz = 50$ K cm^{-1}.

Normalizing according to (2.5), the right and left eigenfunctions are

$$\xi^R_{\nu,k_\parallel n}(z)=\xi^L_{\nu,k_\parallel n}(z)=\frac{k_\parallel}{2\pi}\left(\frac{2}{d}\right)^{1/2} I_n(z) \qquad (n=1,2,3,\ldots) \tag{4.4}$$

with

$$I_n(z)=\begin{cases}\cos k_n z & (n=1,3,5,\ldots)\\ \sin k_n z & (n=2,4,6,\ldots)\end{cases} \tag{4.5}$$

Next we turn to the visco-heat modes. The right modes obey the system (2.6), while the left modes obey the adjoint system (A13). At this point it is convenient to introduce dimensionless quantities as follows:

$$\begin{gathered}\zeta=\frac{z}{d}\quad\left(-\frac{1}{2}\leqslant\zeta\leqslant\frac{1}{2}\right); \qquad W_n(\zeta)=v^R_{\lambda,k_\parallel n}(z)\\ a=k_\parallel d, \qquad \sigma_n=s_{\lambda,k_\parallel n}\frac{d^2}{\nu}\\ P=\frac{\nu}{D_T} \qquad \text{(Prandtl number)}\\ R=-\frac{\alpha g}{\nu D_T}\frac{dT}{dz}d^4 \qquad \text{(Rayleigh number)}\end{gathered} \tag{4.6}$$

Putting also

$$\Theta_n(\zeta)=\left(a^2-\frac{d^2}{d\zeta^2}-\sigma_n\right)\left(a^2-\frac{d^2}{d\zeta^2}\right)W_n(\zeta) \tag{4.7}$$

so that, according to (2.6), $T^R_{\lambda,k_\parallel n}(z)$ is proportional to $\Theta_n(\zeta)$, the Eqs. (2.6) take the form

$$\begin{pmatrix}\frac{1}{P}\left(a^2-\frac{d^2}{d\zeta^2}\right) & -\frac{Ra^2}{P}\\ -1 & \left(a^2-\frac{d^2}{d\zeta^2}\right)^2\end{pmatrix}\begin{pmatrix}\Theta_n\\ W_n\end{pmatrix}=\sigma_n\begin{pmatrix}\Theta_n\\ \left(a^2-\frac{d^2}{d\zeta^2}\right)W_n\end{pmatrix} \tag{4.8}$$

In Appendix B it is shown that the left eigenvalue problem has the same form, except that σ_n must be replaced by σ_n^*. Since the coefficients a, R, and P are all real, it follows that $v^L_{\lambda,k_\parallel n}$ and $T^L_{\lambda,k_\parallel n}$ are proportional to W_n^* and Θ_n^*, respectively. Hence, using (2.7) we can normalize such that

$$\int_{-1/2}^{1/2}\left[W_n W_m+\frac{1}{a^2}\frac{dW_n}{d\zeta}\frac{dW_m}{d\zeta}+\frac{P}{Ra^4}\Theta_n\Theta_m\right]d\zeta=\delta_{nm} \tag{4.9}$$

In this normalization, the eigenvalues and the components of the right and left eigenvectors of the visco-heat modes, expressed in terms of σ_n, $W_n(\zeta)$, and $\Theta_n(\zeta)$, read

$$s_{\lambda,k_\parallel n} = \frac{\nu}{d^2}\sigma_n \tag{4.10a}$$

$$\begin{aligned} T^R_{\lambda,k_\parallel n}(z) &= \frac{\nu}{\alpha g d^2}\frac{1}{a^2}\Theta_n\left(\frac{z}{d}\right) \\ v^R_{\lambda,k_\parallel n}(z) &= W_n\left(\frac{z}{d}\right) \end{aligned} \tag{4.10b}$$

$$\begin{aligned} T^L_{\lambda,k_\parallel n}(z) &= -\frac{1}{(2\pi)^2 d}\frac{\nu}{(dT/dz)\,d^2}\frac{1}{a^2}\Theta^*_n\left(\frac{z}{d}\right) \\ v^L_{\lambda,k_\parallel n}(z) &= \frac{1}{(2\pi)^2 d}W^*_n\left(\frac{z}{d}\right) \end{aligned} \tag{4.10c}$$

The right and the left eigenvalue equations for the visco-heat modes have now both been reduced to the eigenvalue equations (4.8). These have still to be supplemented by the boundary conditions

$$\begin{aligned} &\Theta_n = 0 \\ &W_n = 0 \qquad \frac{dW_n}{d\zeta} = 0 \end{aligned} \qquad (\zeta = \pm 1/2) \tag{4.11}$$

The condition on Θ_n, which is essentially the temperature $T^R_{\lambda,k_\parallel n}$, expresses the ideal heat conductivity of the plates; the two conditions on W_n, which is the z component of the transversal part of the flow velocity $\mathbf{u}^{R,(1)}_{\lambda,\mathbf{k}_\parallel n}$, follow from the stick condition $\mathbf{u}^R_{\lambda,\mathbf{k}_\parallel n} = 0$ at $z = \pm d/2$ together with $\nabla \cdot \mathbf{u}^R_{\lambda,\mathbf{k}_\parallel n} = 0$.

In order to solve the eigenvalue problem (4.8), (4.11) we first eliminate Θ_n between Eqs. (4.8) to obtain the sixth-order differential equation[7]

$$\left(a^2 - \frac{d^2}{d\zeta^2} - P\sigma_n\right)\left(a^2 - \frac{d^2}{d\zeta^2} - \sigma_n\right)\left(a^2 - \frac{d^2}{d\zeta^2}\right) W_n(\zeta) = Ra^2 W_n(\zeta) \tag{4.12}$$

The eigenvalue problem (4.12), (4.11) has been discussed by Chandrasekhar[11] for the special case of $\sigma_n = 0$ in connection with the convective instability. Then (4.12) defines an eigenvalue problem for R at

[7] Hence the six boundary conditions (4.11) are indeed necessary and sufficient to define a well-posed eigenvalue problem.

given a. Here, we are interested, however, in the eigenvalues σ_n for given a and R. We will now briefly sketch how the eigenvalue problem (4.12), (4.11) is solved.[14,8]

From the symmetry of the problem follows that the eigenfunctions $W_n(\zeta)$ possess a definite parity. We make the ansatz

$$W(\zeta) = \begin{cases} \sum_{j=1,2,3} A_j^E \cos q_j \zeta & \text{(even)} \\ \sum_{j=1,2,3} A_j^0 \sin q_j \zeta & \text{(odd)} \end{cases} \tag{4.13}$$

where A_j^E and A_j^0 $(j=1, 2, 3)$ are constants and the $q_j = q_j(\sigma)$ $(j=1, 2, 3)$ are the three roots of the sixth-order equation

$$(a^2+q^2-P\sigma)(a^2+q^2-\sigma)(a^2+q^2) = Ra^2 \tag{4.14}$$

which lie in the right half of the complex plane, i.e., for which $-\pi/2 < \arg q_j \leqslant \pi/2$, with σ considered as a parameter. Functions of the form (4.13) are clearly solutions of (4.12) for any choice of the constants A_j. Applying now the boundary conditions (4.11) yields a homogeneous system of equations for the constants. For the even eigenfunctions this system reads

$$\begin{pmatrix} \cos\frac{q_1}{2} & \cos\frac{q_2}{2} & \cos\frac{q_3}{2} \\ q_1 \sin\frac{q_1}{2} & q_2 \sin\frac{q_2}{2} & q_3 \sin\frac{q_3}{2} \\ (Q_1-\sigma)\, Q_1 \cos\frac{q_1}{2} & (Q_2-\sigma)\, Q_2 \cos\frac{q_2}{2} & (Q_3-\sigma)\, Q_3 \cos\frac{q_3}{2} \end{pmatrix} \begin{pmatrix} A_1^E \\ A_2^E \\ A_3^E \end{pmatrix} = 0 \tag{4.15}$$

where we have set $Q_j = a^2 + q_j^2$ $(j=1, 2, 3)$. For the odd eigenfunctions one obtains a similar system with sin and cos interchanged. Nontrivial solutions of (4.15), and thus nonvanishing $W(\zeta)$, exist only when the determinant of the 3×3 matrix in (4.15), $F^E(\sigma; a, R)$, is zero. For fixed a and R the characteristic equation

$$F^E(\sigma; a, R) = 0 \tag{4.16}$$

has an infinite number of solutions σ. These are the eigenvalues of the even modes. Similarly one computes the eigenvalues of the odd modes by solving the corresponding characteristic equation $F^0(\sigma; a, R) = 0$. In this way one obtains all the eigenvalues

$$\sigma = \sigma_n(a, R) \tag{4.17}$$

where the discrete index n labels the modes for fixed a and R. We remark that σ_n also depends on the Prandtl number P. However, we will not indicate this explicitly.

In order to compute the eigenfunction $W_n(\zeta)$ corresponding to σ_n, one inserts the three (complex) wave numbers $q_{nj}(a, R) = q_j(\sigma_n)$ $(j = 1, 2, 3)$ into (4.13). If $W_n(\zeta)$ is an even eigenfunction, two of the three constants $A_{nj}(a, R) = A_j^E(\sigma_n)$ follow from (4.15). If $W_n(\zeta)$ is odd, one must use the equations corresponding to (4.15) for the odd modes to determine two of the three constants $A_{nj}(a, R) = A_j^0(\sigma_n)$. After $\Theta_n(\zeta)$ has been calculated from (4.7), one must determine the third constant from the normalization condition (4.9). This completes the computation of the eigenmodes for the eigenvalue problem (4.8), (4.11) of the visco-heat modes.

Inserting Eqs. (4.2)–(4.5) and (4.10), with σ_n, $W_n(\zeta)$ and $\Theta_n(\zeta)$ being computed in the way described above, into Eqs. (2.8)–(2.12) gives explicit expressions for $\mathsf{M}^{(sl)}$. The actual calculation of the visco-heat modes with stick boundary conditions is complicated, however. In particular, the characteristic equations [cf. Eq. (4.16)] can only be solved numerically. Therefore we will postpone the calculation of $\mathsf{M}^{(sl)}$ for a number of cases to Sections 6 and 7, and mention first some general properties of the visco-heat modes.

5. VISCO-HEAT MODES FOR STICK BOUNDARY CONDITIONS

In this section we will discuss the behavior of the visco-heat modes for stick boundary conditions and fixed reduced wave number a as a function of the Rayleigh number R.[8] We will illustrate the discussion by a few numerical examples.

Before studying the exact eigenvalues $\sigma_n(R)$, it is useful first to consider a simple approximation, namely, the parabolic approximation.[15] This approximation describes the eigenvalues σ_n reasonably well for many R, with the exception of one qualitatively and quantitatively important feature, that we will discuss below.

5.1. Parabolic Approximation

For the parabolic approximation of the eigenvalues $\sigma_n(R)$ we consider for fixed a the (R, σ) plane. Then for each n, $\sigma_n(R)$ is approximated by a branch of a parabola through three special points in the plane, that are exact solutions of the eigenvalue problem. These points are $(0, \sigma_{nv})$,

[8] We will suppress the dependence of σ_n on a in this section.

$(0, \sigma_{nH})$ and $(R_{nC}, 0)$ where σ_{nv} and σ_{nH} are the eigenvalues of the nth viscous and heat mode, respectively, in equilibrium (when $R=0$), and $R_{nC}>0$ is the solution of the equation $\sigma_n(R)=0$, considered by Chandrasekhar.[11] Expressions, which determine the dependence of σ_{nv}, σ_{nH}, and R_{nC} on the wave number a, are given in Appendix C. In parabollic approximation the eigenvalues are thus

$$\sigma_{n\pm}(R)=\frac{\sigma_{nv}+\sigma_{nH}}{2}\pm\frac{\sigma_{nv}-\sigma_{nH}}{2}\times\left[1+\frac{4\sigma_{nv}\sigma_{nH}}{(\sigma_{nv}-\sigma_{nH})^2}\frac{R}{R_{nC}}\right]^{1/2} \qquad (n=1, 2, 3,...) \qquad (5.1)$$

We remark that relations of the form (5.1) are exact for the mathematically simpler slip boundary conditions, where $\sigma_{nv}=a^2+n^2\pi^2$, $\sigma_{nH}=(1/P)(a^2+n^2\pi^2)$ and $R_{nC}=(a^2+n^2\pi^2)^3/a^2$ [16,10,8] [cf. also Eq. (3.5) with k_z being replaced by $k_n=n(\pi/d)$].

The eigenvalues $\sigma_{n\pm}(R)$, as given by Eq. (5.1) in parabolic approximation, are analytic functions of R with no singularities except at the branch points (R_{nB}, σ_{nB}), where $R_{nB}=-(\sigma_{nv}-\sigma_{nH})^2R_{nC}/(4\sigma_{nv}\sigma_{nH})$ and $\sigma_{nB}=(\sigma_{nv}+\sigma_{nH})/2$. We note that the functions $\sigma_{n\pm}(R)$ are still continuous at $R=R_{nB}$ and that for $R>R_{nB}$ the approximate eigenvalues $\sigma_{n+}(R)$ and $\sigma_{n-}(R)$ are both real, while for $R<R_{nB}$ they are complex conjugate.

5.2. Propagating Modes

A mode with a real eigenvalue is diffusive and decays exponentially.[9] On the other hand, a mode with a complex eigenvalue propagates, while it is damped.[8] Both types of time evolution are physically possible for the nonequilibrium visco-heat modes, owing to the interplay of the buoyancy force, which is caused by the gravity field, and the driving force, which is caused by the heat flux. We have elaborated this elsewhere.[8] Propagation can only occur when the system is heated from above ($R<0$), since then the driving force opposes the buoyancy force. Mathematically this follows directly from (4.8) since σ_n is real for $R>0$, as is shown in Ref. 14 and in Appendix B. Experimentally, propagating visco-heat modes have been observed by Allain *et al.*[15,17] using forced-Rayleigh-scattering spectroscopy.

[9] We assume that all the eigenvalues are positive, or have a positive real part. This is the case as long as the stationary state is stable (see beginning of next section).

5.3. Exact Results

In order to discuss the behavior of the exact eigenvalues we have solved the characteristic equation (4.16) numerically for the first few even eigenvalues $\sigma = \sigma_n(R)$ in a few examples. We have chosen the Prandtl number $P = 2$ and the wave numbers $a = 2$, 4, 6, 8, and 10, respectively. The results are plotted in Figs. 1a–e. The thick lines denote the exact results, while the thin lines refer to the parabolic approximation, i.e., the curves $1+$, $1-$, $3+$, $3-$, and $5-$ as obtained from (5.1). The dashed lines indicate the real part of the complex eigenvalues.

One recognizes from these figures that the parabolic approximation describes the eigenvalues reasonably well in wide parts of the (R, σ) plane. Striking deviations occur, however, in the neighborhood of the so-called "crossing points" where parabolas of different order n cross. The exact curves avoid the crossing when they are of equal parity. This is the important difference between the exact eigenvalues and the parabolic approximation mentioned at the beginning of this section. Modes with different parity can

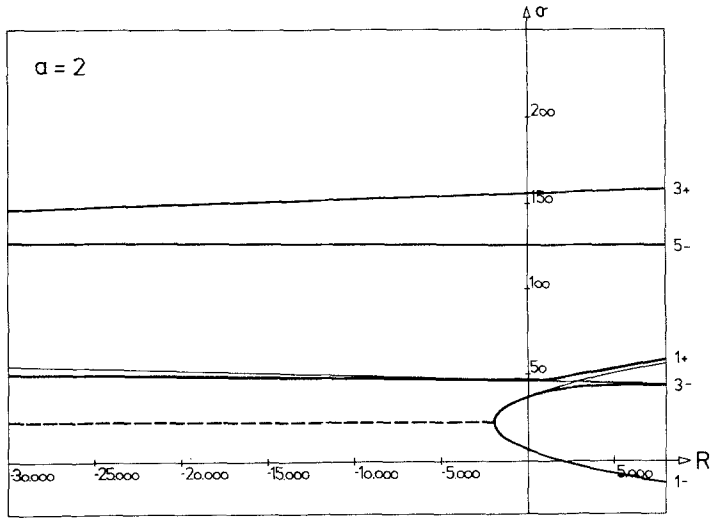

(a)

Fig. 1. Eigenvalues $\sigma_n(R)$ of the visco-heat modes for the first few even eigenmodes as functions of R. In all five plots the Prandtl number $P = 2$. The horizontal wave numbers are as follows: Fig. 1a, $a = 2$; Fig. 1b, $a = 4$; Fig. 1c, $a = 6$; Fig. 1d, $a = 8$; Fig. 1e, $a = 10$. The meaning of the various types of lines is: ——, real eigenvalues (exact results); – – –, real part of complex eigenvalues (exact); ——, real eigenvalues in parabolic approximation (5.1); – – – –, real part of complex eigenvalues (parabolic approximation). Notice that the exact curves avoid to cross, in contrast to the parabolic curves.

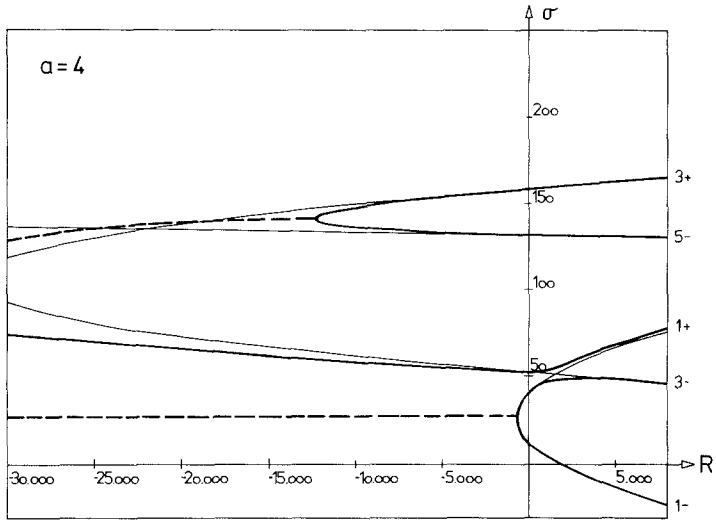

(b)

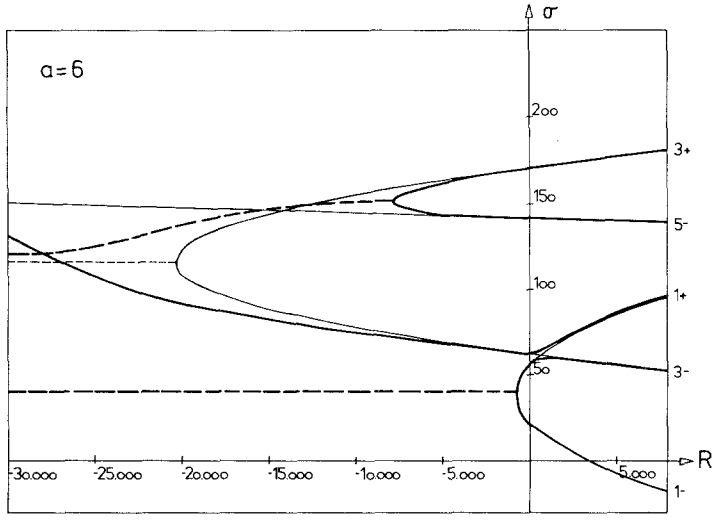

(c)

Fig. 1 (*continued*)

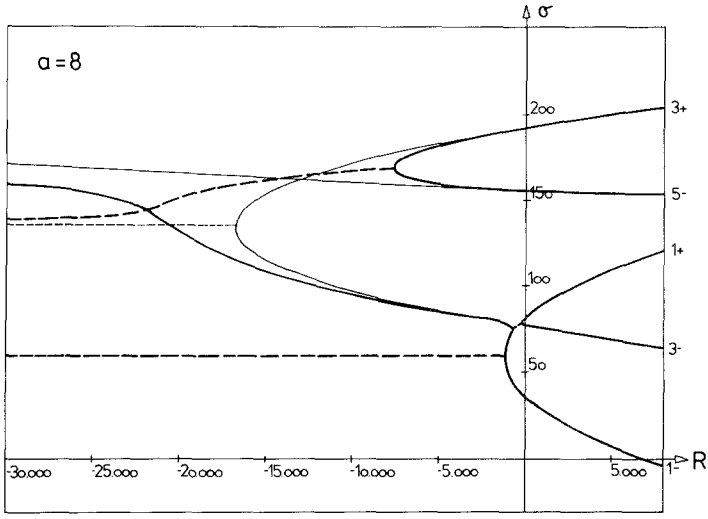

(d)

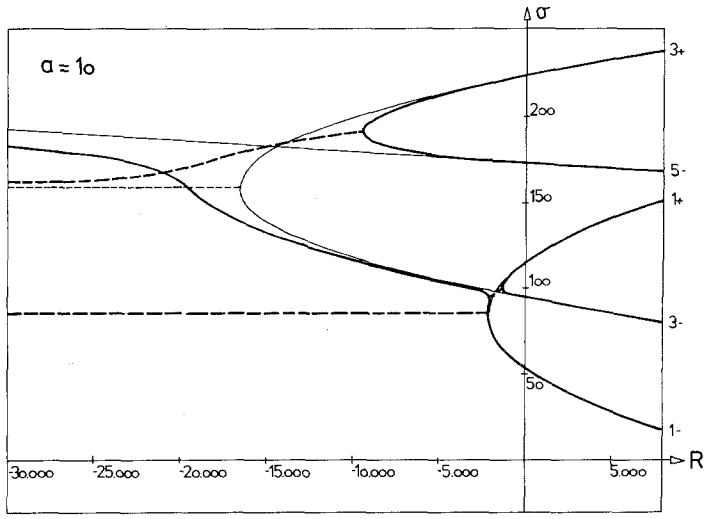

(e)

Fig. 1 (*continued*)

cross without affecting each other. The advoidance of crossing is accomplished in one out of two ways: For $R \geqslant 0$, when the eigenvalues are real, the two modes have to pass horizontally in the (R, σ) plane, while for $R < 0$ they appear to pass always vertically since they can become complex (Fig. 1). In the latter case the exact branch points may be shifted considerably away from the positions they have in parabolic approximation. In Table I we have listed the numerical values for the exact positions (R_B, σ_B) of the branch points appearing in Fig. 1 and compared them with the values obtained in parabolic approximation. Those branch points, where the parabolic approximation fails badly in our examples are caused due to the crossing of the parabolas $3+$ and $5-$, forcing the exact modes to pass vertically before this crossing point is reached. Thereby branch points are generated with values of R_B much lower than those expected from the parabolic approximation, where the branch points are just the vertex point of the parabolas $\sigma_{3\pm}(R)$.

Moreover, pairs of new branch points appear, which frame certain "windows of propagation," such as the behavior near the crossing point $(1+, 3-)$ in the examples $a = 8$ and $a = 10$ shows. In Fig. 2 we have plotted a close-up of this window in the case $a = 8$.

Because of the complications caused by the avoidance of crossing, one can order the eigenvalues only at fixed R. Orderings at different R cannot be uniquely connected through a branch point.

5.4. Mathematical Behavior near the Branch Points

We will end this section with a few mathematical remarks on the behavior of the eigenvalues and eigenprojections near the branch points, based on some theorems proven in Kato's book.[18]

(i) Two eigenvalues $\sigma_n(R)$ and $\sigma_m(R)$ which meet in a branch point (R_0, σ_0) can be represented by the Puiseux series[18]

$$\sigma_{\pm}(R) = \sigma_0 \pm \alpha_1 (R - R_0)^{1/2} + \alpha_2 (R - R_0) \pm \alpha_3 (R - R_0)^{3/2} + \cdots \quad (5.2)$$

in a neighborhood of R_0, where $\alpha_1, \alpha_2, \alpha_3, \ldots$ are constants. Branch points are the only points where the eigenvalues $\sigma_n(R)$ are not analytic functions.

(ii) The eigenprojections $\mathscr{P}_n$ and $\mathscr{P}_m$ corresponding to σ_n and σ_m, respectively (they are defined more explicitly in Appendix B) behave near R_0 like

$$\mathscr{P}_{\pm}(R) = \pm \mathscr{N}_0 (R - R_0)^{-1/2} + \tfrac{1}{2}\mathscr{P}_0 + \cdots \quad (5.3)$$

where $\mathscr{P}_0$ is the total projection operator corresponding to σ_0 and $\mathscr{N}_0$ is a nilpotent operator, i.e., $\mathscr{N}_0^2 = 0$. Since $\mathscr{P}_{\pm}^2 = \mathscr{P}_{\pm}$ and $\mathscr{P}_+ \mathscr{P}_- = 0$ it follows furthermore that $\mathscr{P}_{\pm} \mathscr{N}_0 = \mathscr{N}_0 \mathscr{P}_{\pm} = \mathscr{N}_0$.

Table I. Comparison of the Values for the Branch Points Appearing in Figs. 1a–e as Obtained from an Exact Calculation and from the Parabolic Approximation

a	(R_B, σ_B) [Parabolic approx.]			
2	(−2 016.0, 22.2) [(−1 944.0, 22.1)]			
4	(−705.0, 27.5) [(−688.0, 26.8)]	(−12 353.0, 142.0) [(−31 874.0, 106.0)]		
6	(−731.6, 39.5) [(−715.4, 39.2)]	(−7 851.0, 152.0) [(−20 347.0, 117.0)]		
8	(−171.0, 77.9) [(—)]	(−708.0, 74.9) [(—)]	(−1 172.0, 59.4) [(−1 143.0, 58.8)]	(−7 778.0, 169.0) [(−16 868.0, 135.0)]
10	(−1 297.0, 100.0) [(—)]	(−2 069.0, 92.9) [(—)]	(−2 034.0, 80.8) [(−2 030.0, 85.0)]	(−9 499.0, 191.0) [(−16 543.0, 159.0)]

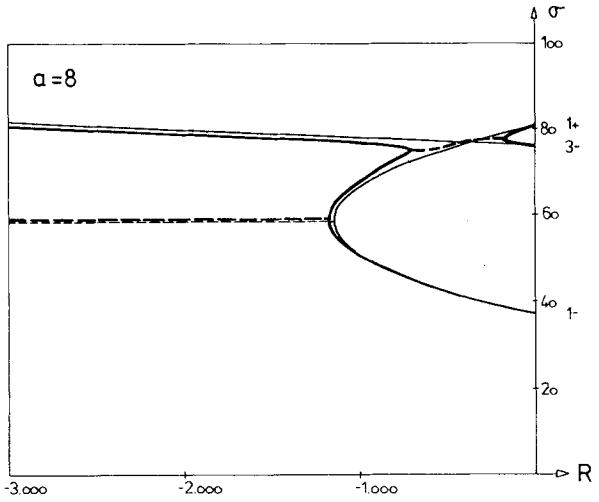

Fig. 2. Close-up of the "window of propagation" from Fig. 1d.

(iii) Combining (5.2) and (5.3) one sees that $\sigma_+ \mathscr{P}_+ + \sigma_- \mathscr{P}_-$, i.e., the nonanalytic part of the Jordan representation of the operator in (4.8) defining the visco-heat modes, is continuous in R_0. The merging of two modes in a branch point (R_0, σ_0) gives rise to generalized eigenmodes that do not evolve exponentially with time τ, but like $\tau e^{-\sigma_0 \tau}$.

The proofs for Eqs. (5.2) and (5.3) given by Kato are mere existence proofs. Explicit expressions for the constants $\alpha_1, \ldots$ and the operators $\mathscr{N}_0$ and $\mathscr{P}_0$ can only be given when the details of the eigenmodes near the branch point are known. Therefore we illustrate the formal results in Appendix D for the case of slip boundary conditions, where all the quantities can be determined explicitly.

From the above considerations follows that the integrands appearing in the correlation functions (2.8) (the sums over n being understood to be part of the integrands) are continuous functions of the Rayleigh number R in the branch points. Hence, the correlation matrix $\mathsf{M}^{(sl)}$ is a continuous function of R away from the convective instability. $\mathsf{M}^{(sl)}$ becomes singular at the instability point, because then one of the eigenvalues σ_n vanishes, causing the mode-coupling contributions to (2.9) to diverge. In the next two sections we use the eigenmodes discussed here to study as examples the behavior of $\mathsf{M}^{(sl)}$ near, but below, the convective instability (Section 6), and the Rayleigh line in the scattering of light for very small wave vectors (Section 7).

6. CONVECTIVE INSTABILITY

The stationary state solution $p(z)$, $T(z)$, $\mathbf{u}=0$, around which the fluctuations are discussed here, is unstable when the corresponding hydrodynamic operator has an eigenvalue with a negative real part.[8,11] In this case not every initial perturbation $\delta\mathbf{a}(\mathbf{r}, 0)$ of the laminar steady state will decay to zero as $t \to \infty$, but some will increase exponentially. The system responds to this hydrodynamic instability by performing a transition to convective flow. In this section we will discuss the correlation matrix near the convective instability.

The only hydrodynamic modes to become unstable are the visco-heat modes, since the viscous and the sound modes have a finite damping part for finite d which is proportional to the transport coefficients. In Appendix B we show for the visco-heat modes that $\mathrm{Re}\,\sigma_n > 0$ for all $R \leqslant 0$. Hence, convection can only occur when the fluid is heated from below ($R > 0$). Physically, the convective motion is caused by the buoyancy force which, for $R > 0$, supports the tendency of the hot and light fluid to go up and of the cold and heavy material to go down.[8]

The lowest value of R, for which the real part of one of the eigenvalue relations (4.17) vanishes, is the critical Rayleigh number R_c. We denote that branch of the eigenvalue relations whose real part goes first to zero as R increases, starting from $R=0$, by $\sigma^{(1)}(a, R)$. From Eq. (B20) in Appendix B follows that $\mathrm{Im}\,\sigma^{(1)}(a, R_c)=0$, since $R_c > 0$. This is known as the so-called "principle of exchange of stabilities."[11] The curve of marginal stability, $R = R^{(1)}(a)$, is therefore obtained by inverting the equation $\sigma^{(1)}(a, R)=0$.

In order to compute $R^{(1)}(a)$ we take the characteristic equation (4.16), since the eigenfunction corresponding to the lowest eigenvalue has even parity. Putting $\sigma = 0$ yields

$$F_0(a, R) \equiv F^E(0; a, R) = 0 \tag{6.1}$$

Equation (6.1) has still infinitely many solutions $R = R_n(a)$. The curve of marginal stability $R = R^{(1)}(a)$ is that branch on which the lowest R value is attained. The minimum of $R^{(1)}(a)$ is the instability point (a_c, R_c). Hence it is defined by the equations

$$\left(\frac{dR^{(1)}}{da}\right)_{a=a_c} = 0, \qquad R_c = R^{(1)}(a_c) \tag{6.2}$$

We remark that a_c and R_c do not depend on the Prandtl number since $F_0(a, R)$ is independent of P. Numerical results for a_c and R_c have been obtained long ago (see Ref. 11 and references therein).

After the instability point has been determined, we investigate next the behavior of the visco-heat modes close to the instability point. This will enable us to compute the correlation matrix in the limit where the instability is approached from below, i.e., as $R \to R_{c-}$.

Expanding $\sigma^{(1)}$ around (a_c, R_c) yields

$$\sigma^{(1)}(a, R) = \Gamma_P \left[1 - \frac{R}{R_c} + \Lambda^2 \frac{(a-a_c)^2}{a_c^2} \right] + \cdots \qquad (R \to R_{c-}; a \approx a_c) \tag{6.3}$$

where

$$\Gamma_P = -R_c \left(\frac{\partial \sigma^{(1)}}{\partial R} \right)_{a_c, R_c}, \qquad \Lambda^2 = \frac{a_c^2}{2R_c} \left(\frac{d^2 R^{(1)}}{da^2} \right)_{a_c} \tag{6.4}$$

and where (6.2) has been used. From (6.4) follows that Λ^2 is determined from the curvature of the curve $R^{(1)}(a)$ in the instability point. To compute Γ_P,[10] one expands the characteristic function $F^E(\sigma; a, R)$ to first order in σ:

$$F^E(\sigma; a, R) = F_0(a, R) + \sigma F_1(a, R) + \cdots \tag{6.5}$$

where $F_1 = (\partial F^E / \partial \sigma)_{\sigma=0}$. From (4.16) and (6.3) follows then

$$\Gamma_P = \frac{R_c}{F_1(a_c, R_c)} \left(\frac{\partial F_0}{\partial R} \right)_{a_c, R_c} \tag{6.6}$$

Wesfreid *et al.*[19] have computed the values of Γ_P and Λ^2 and verified their results experimentally by measuring the decay rate of the critical mode near the instability (i.e., the so-called critical slowing down) with the aid of forced-Rayleigh-scattering techniques.

We need also the components of the normalized eigenvectors for $a = a_c$ and $R = R_c$, which we denote by $W_c(\zeta)$ and $\Theta_c(\zeta)$. Since the instability point is not a branch point,[11] it follows from the discussion in Section 5d that $W_c(\zeta)$ and $\Theta_c(\zeta)$ are analytic functions of ζ. They can be determined in the manner outlined below Eq. (4.17).

We can now compute the correlation functions near the instability according to Eqs. (2.8)–(2.10). For $R = R_c$ the correlation functions diverge, since $\sigma^{(1)}(a_c, R_c) = 0$. As $R \to R_{c-}$, their magnitude is dominated by the eigenvalues $\sigma^{(1)}(a, R)$ in the vicinity of the instability point, given by (6.3), and all the local equilibrium contributions are negligible since they

[10] The index P denotes that this quantity depends on the Prandtl number P.

[11] This is clear since, according to Section 5.2, branch points can only occur for $R \leqslant 0$ while the instability arises at $R = R_c > 0$.

stay finite. To be more quantitative, we introduce the positive dimensionless parameter

$$\varepsilon = \frac{a_c}{\Lambda}\left(1 - \frac{R}{R_c}\right)^{1/2} \tag{6.7}$$

Then, in the regime $\varepsilon \ll a_c$, the only mode-coupling coefficient (2.10), which contributes to the singular behavior of the correlation functions, is found with the aid of (4.10) to be

$$\Lambda_{cc} = -2\frac{T}{\rho}\frac{\nu}{d^2}\frac{1}{(2\pi)^4 d^2}\Upsilon_P \tag{6.8}$$

where

$$\Upsilon_P = \frac{1}{a_c^2}\int_{-1/2}^{1/2} W_c(\zeta)\,\Theta_c(\zeta)\,d\zeta \tag{6.9}$$

In terms of the dimensionless variables

$$\begin{gathered}\zeta_1 = z_1/d, \qquad \zeta_2 = z_2/d, \qquad \xi = r_{\|}/d \\ \tau = \frac{\nu}{d^2}\frac{\Gamma_P \Lambda^2}{a_c^2}\,t\end{gathered} \tag{6.10}$$

we thus obtain from (2.8), (2.9), and (6.8) for $\varepsilon \ll a_c$

$$\begin{aligned} S(r_{\|}, z_1, z_2; t) &= k_B \frac{c_p^2}{\rho T}\frac{\nu^2}{\alpha^2 g^2 d^7} K_P G_\varepsilon(\xi, \tau)\,\Theta_c(\zeta_1)\,\Theta_c(\zeta_2) \\ S'(r_{\|}, z_1, z_2; t) &= k_B \frac{c_p}{\rho}\frac{\nu}{\alpha g d^3} K_P G_\varepsilon(\xi, \tau)\,\Theta_c(\zeta_1)\,W_c(\zeta_2) \\ V(r_{\|}, z_1, z_2; t) &= k_B \frac{T}{\rho}\, d K_P\, G_\varepsilon(\xi, \tau)\,W_c(\zeta_1)\,W_c(\zeta_2) \qquad (\varepsilon \ll a_c) \end{aligned} \tag{6.11}$$

where

$$K_P = \frac{\Upsilon_P}{\Gamma_P \Lambda^2 a_c^2} \tag{6.12}$$

and

$$G_\varepsilon(\xi, \tau) = \frac{1}{2\pi}\, e^{-\varepsilon^2 \tau}\int_0^\infty a J_0(a\xi)\frac{e^{-(a-a_c)^2\tau}}{(a-a_c)^2 + \varepsilon^2}\,da \tag{6.13}$$

It is this function $G_\varepsilon(\xi, \tau)$, appearing in all three correlation functions (6.11), that diverges in the limit $\varepsilon \to 0$ for all distances ξ and times τ.

Inserting (6.11) into (2.11), (2.12) one can straightforwardly compute $\mathsf{M}^{(\mathrm{sl})}(\mathbf{r}_1, t_1; \mathbf{r}_2, t_2)$ in the limit $R \to R_{c-}$. Therein the contribution from the viscous modes, i.e., Ξ, is negligible, since it is a local equilibrium quantity and thus stays finite as $R \to R_{c-}$. Even the fast part of the correlation matrix, which is generated by the sound modes (and which will be considered in paper III), stays finite at $R = R_c$, since all the sound modes have a positive real, i.e., a damping, part. Therefore the fast part of M does not contribute to the singular behavior of the hydrodynamic correlation matrix near the instability either, and we may drop the superscript (sl). For general distances and times, the expressions thus obtained for $\mathsf{M}(\mathbf{r}_1, t_1; \mathbf{r}_2, t_2)$ in the limit $R \to R_{c-}$ are still rather lengthy and will not be given here. Instead we will restrict ourselves in the following to a discussion of the large-distance behavior as $r_{\|} \to \infty$.

Using that the integrand in (6.13) is sharply peaked around a_c one can straightforwardly evaluate the function $G_\varepsilon(\xi, \tau)$ for large horizontal distances $\xi \gg a_c^{-1}$. The result is

$$G_\varepsilon(\xi, \tau) = \left(\frac{a_c}{2\pi\xi}\right)^{1/2} Z_\varepsilon(\xi, \tau) \cos\left(a_c \xi - \frac{\pi}{4}\right) \qquad (\xi \gg a_c^{-1}) \quad (6.14)$$

where[20]

$$Z_\varepsilon(\xi, \tau) = \frac{1}{\pi} e^{-\varepsilon^2 \tau} \int_{-\infty}^{\infty} \frac{e^{-a^2\tau}}{a^2 + \varepsilon^2} \cos a\xi \, da$$

$$= \frac{1}{2\pi}\left[e^{-\varepsilon\xi} \operatorname{erfc}\left(\varepsilon\sqrt{\tau} - \frac{\xi}{2\sqrt{\tau}}\right) + e^{\varepsilon\xi} \operatorname{erfc}\left(\varepsilon\sqrt{\tau} + \frac{\xi}{2\sqrt{\tau}}\right)\right] \quad (6.15)$$

and

$$\operatorname{erfc}(x) = 1 - \frac{2}{\sqrt{\pi}} \int_0^x e^{-t^2} \, dt \quad (6.16)$$

is the complementary error function.

Inserting now (6.11) and (6.14) into (2.11), (2.12) and keeping only the divergent terms[12] we obtain

$$M_{TT}(\mathbf{r}_1, t_1; \mathbf{r}_2, t_2)$$

$$= k_B \frac{T}{\rho} \frac{v^2}{\alpha^2 g^2 d^7} K_P \left(\frac{a_c}{2\pi\xi}\right)^{1/2} Z_\varepsilon(\xi, \tau) \cos\left(a_c \xi - \frac{\pi}{4}\right) \Theta_c(\zeta_1) \, \Theta_c(\zeta_2)$$

[12] From (6.15) follows that $Z_\varepsilon(\xi, \tau) = O(1/\varepsilon)$ while $(\partial/\partial\xi) Z_\varepsilon(\xi, \tau) = O(1)$.

$$\mathbf{M}_{Tu}(\mathbf{r}_1, t_1; \mathbf{r}_2, t_2)$$
$$= k_B \frac{T}{\rho} \frac{\nu}{\alpha g d^5} K_P a_c \left(\frac{a_c}{2\pi\xi}\right)^{1/2} Z_\varepsilon(\xi, \tau)$$
$$\times \left[\cos\left(a_c\xi - \frac{\pi}{4}\right) a_c \Theta_c(\zeta_1)\, W_c(\zeta_2)\, \mathbf{e}_z \right.$$
$$\left. + \sin\left(a_c\xi - \frac{\pi}{4}\right) \Theta_c(\zeta_1) \frac{dW_c}{d\zeta_2} \hat{\mathbf{r}}_\parallel \right]$$

$$\mathbf{M}_{uu}(\mathbf{r}_1, t_1; \mathbf{r}_2, t_2)$$
$$= k_B \frac{T}{\rho} \frac{1}{d^3} K_P a_c^2 \left(\frac{a_c}{2\pi\xi}\right)^{1/2} Z_\varepsilon(\xi, \tau) \left\{ \cos\left(a_c\xi - \frac{\pi}{4}\right) \right.$$
$$\times \left[a_c^2 W_c(\zeta_1)\, W_c(\zeta_2)\, \mathbf{e}_z\mathbf{e}_z + \frac{dW_c}{d\zeta_1}\frac{dW_c}{d\zeta_2} \hat{\mathbf{r}}_\parallel\hat{\mathbf{r}}_\parallel + a_c \sin\left(a_c\xi - \frac{\pi}{4}\right) \right]$$
$$\left. \times \left[W_c(\zeta_1) \frac{dW_c}{d\zeta_2} \mathbf{e}_z\hat{\mathbf{r}}_\parallel - \frac{dW_c}{d\zeta_1} W_c(\zeta_2)\, \hat{\mathbf{r}}_\parallel\mathbf{e}_z \right] \right\} \qquad (\varepsilon \ll a_c;\ \xi \gg a_c^{-1}) \quad (6.17)$$

From (6.17) one can derive, in particular, expressions for short and long times $t = t_1 - t_2 \gtrsim 0$ by evaluating the function $Z_\varepsilon(\xi, \tau)$, defined in (6.15), asymptotically. Assuming that $\xi \gtrsim \varepsilon^{-1}$, one finds[21]

$$Z_\varepsilon(\xi, \tau) = \begin{cases} \dfrac{1}{\varepsilon} e^{-\varepsilon\xi} & \left(\dfrac{\tau}{\xi} \ll \dfrac{1}{\varepsilon}\right) \\ \dfrac{1}{\varepsilon^2} \cosh \varepsilon\xi \dfrac{e^{-\varepsilon^2\tau}}{(\pi\tau)^{1/2}} & \left(\dfrac{\tau}{\xi} \gg \dfrac{1}{\varepsilon}\right) \end{cases} \qquad (6.18)$$

For short times, i.e., $\tau/\xi \ll 1/\varepsilon$, the correlation matrix is thus independent of τ,[13] and its long-distance decay in horizontal direction can be characterized by a dimensionless correlation length

$$\xi_c = \frac{1}{\varepsilon} = \frac{\Lambda}{a_c} \frac{1}{\sqrt{1 - R/R_c}} \qquad (6.19)$$

where (6.7) has been used. The long-time behavior, on the other hand, can be described by a dimensionless correlation time

$$\tau_c = \frac{1}{\varepsilon^2} = \frac{\Lambda^2}{a_c^2} \frac{1}{1 - R/R_c} \qquad (6.20)$$

Both, ξ_c and τ_c, go to infinity as R approaches R_c.

[13] The condition $\tau/\varepsilon \ll 1/\varepsilon$ means physically that the times considered are much smaller than the time ξ^2 it takes an initial fluctuation, localized in the origin, to spread over the distance ξ. Hence one should expect to find just the equal-time correlation matrix.

It is clear from the derivation that expressions of the form (6.11) and (6.17) for the correlation matrix near the instability hold for arbitrary boundary conditions, as long as the visco-heat modes have a discrete spectrum. For the temperature-temperature correlation function this has first been shown by Zaitsev and Shliomis.[9] These authors have also obtained the formulas (6.19) and (6.20) for the correlation length and the correlation time, respectively. Without reference to any specific boundary conditions, the values of the constants R_c, a_c, A^2, Γ_P, K_P and the functions $W_c(\zeta)$, $\Theta_c(\zeta)$ are still undetermined, however.

Finally, we quote the numerical values of these quantities for stick boundary conditions. They are

$$R_c \approx 1707.762, \qquad a_c \approx 3.117$$

$$A^2 \approx 1.46, \qquad \Gamma_P \approx \frac{38.3}{1+2.03P}, \qquad K_P \approx 0.0706\,\frac{1+2.03P}{1+1.96P}$$

$$W_c(\zeta) = N_P[\cos q_0\zeta + 2\,\mathrm{Re}\,A_+ \cos q_+\zeta]$$

$$\Theta_c(\zeta) = \left(a_c^2 - \frac{d^2}{d\zeta^2}\right)^2 W_c(\zeta) \tag{6.21}$$

$$q_0 \approx 3.974, \qquad q_+ \approx 2.126 + 5.195i$$

$$A_+ \approx (-3.077 + 5.195i)\times 10^{-2}$$

$$N_P^2 \approx \frac{1.25}{1+1.96P}$$

While most of these values have been obtained before in the literature,[11,19] the values of N_P and K_P are new. For comparison we quote here also the results for slip boundary conditions[10]:

$$R_c = \frac{27}{4}\pi^4 \approx 657.51, \qquad a_c = \frac{\pi}{\sqrt{2}} \approx 2.221$$

$$A^2 = \frac{4}{3} \approx 1.33, \qquad \Gamma_P = \frac{3\pi^2}{2(1+P)} \approx \frac{14.80}{1+P}, \qquad K_P = \frac{3}{2\pi^4} \approx 0.0154$$

$$W_c(\zeta) = N_P \cos \pi\zeta \tag{6.22}$$

$$\Theta_c(\zeta) = \left(a_c^2 - \frac{d^2}{d\zeta^2}\right)^2, \qquad W_c(\zeta) = \frac{9}{4}\pi^4 W_c(\zeta)$$

$$N_P^2 = \frac{2}{3(1+P)}$$

7. LIGHT-SCATTERING: THE RAYLEIGH LINE

As a second application of our theory for the slow part of the correlation matrix developed in Sections 2–4, we compute the Rayleigh line in the light-scattering spectrum for a number of examples. In simple fluids the spectral intensity of the scattered light is proportional to the dynamic structure factor $S(\mathbf{k}, \omega)$, defined by[2,5]

$$S(\mathbf{k}, \omega) = \frac{1}{V_s T_s} \int_{V_s} \mathbf{d}r_1 \int_{V_s} \mathbf{d}r_2 \int_{-T_s/2}^{T_s/2} dt_1 \times \int_{-T_s/2}^{T_s/2} dt_2 \exp\{-i[\mathbf{k} \cdot (\mathbf{r}_1 - \mathbf{r}_2) - \omega(t_1 - t_2)]\} \times M_{\rho\rho}(\mathbf{r}_1, t_1; \mathbf{r}_2, t_2) \tag{7.1}$$

where

$$M_{\rho\rho}(\mathbf{r}_1, t_1; \mathbf{r}_2, t_2) = \langle \delta\rho(\mathbf{r}_1, t_1)\, \delta\rho(\mathbf{r}_2, t_2) \rangle_{ss} \tag{7.2}$$

is the density–density correlation function in the stationary state. In (7.1) $\mathbf{k}$ and ω are proportional to the transfer of momentum and energy, respectively, from the fluid to the light beam.[2] Finally, V_s is the scattering volume and T_s is the scattering time. We have assumed in (7.1) that the scattering volume is uniformly illuminated during the scattering time and that no light scattered from regions outside V_s will be detected.

For wave vectors $\mathbf{k}$ and frequencies ω in the hydrodynamic regime we may use in (7.1) the result for $M_{\rho\rho}(\mathbf{r}_1, t_1; \mathbf{r}_2, t_2)$, as obtained from a hydrodynamic calculation. The density fluctuations $\delta\rho(\mathbf{r}, t)$ can then be expressed in terms of the pressure and the temperature fluctuations via the linearized thermodynamic relation $\delta\rho = \rho\chi_T\, \delta\rho - \rho\alpha\, \delta T$, where χ_T is the isothermal compressibility.

Here we restrict ourselves to the Rayleigh line of the light-scattering spectrum, which is generated by the slow part of the density–density correlation function only. Using (2.11) and (2.12) one obtains for the slow part of $M_{\rho\rho}$:

$$\begin{aligned} M_{\rho\rho}^{(\mathrm{sl})}(\mathbf{r}_1, t_1; \mathbf{r}_2, t_2) &= \rho^2\alpha^2 M_{TT}^{(\mathrm{sl})}(\mathbf{r}_1, t_1; \mathbf{r}_2, t_2) \\ &= \rho^2\alpha^2 \frac{T^2}{c_p^2} \times \begin{cases} S(r_\parallel, z_1, z_2; t) & (t \geqslant 0) \\ S(r_\parallel, z_2, z_1; -t) & (t < 0) \end{cases} \end{aligned} \tag{7.3}$$

where $S(r_\parallel, z_1, z_2; t)$ is given by the first of Eqs. (2.8a), and (2.13) has been used. In (7.3) we take the values of the average quantities in the center of

the scattering volume, i.e., we choose the z coordinate of the center to be the reference point R_z. As was pointed out in Section 2, Eq. (7.3) is only valid, if $\mathbf{r}_1$ and $\mathbf{r}_2$ both lie inside a horizontal fluid layer around R_z of height $l_0 \ll L_\nabla$ within which the spatial variation of the average quantities can be neglected. In order to ensure that only correlations between such points are probed in (7.1), we will assume in the following that $k_z \gtrsim l_0^{-1}$.

The dynamic structure factor of the Rayleigh line, $S_R(\mathbf{k}, \omega)$, is then found by inserting Eq. (7.3) into (7.1). The expression simplifies when the scattering volume and the scattering time are chosen such that the two sides of the horizontal cross section of the scattering volume are much larger than $k_{\|}^{-1}$, where $\mathbf{k}_{\|} = (\mathbf{1} - \mathbf{e}_z \mathbf{e}_z) \cdot \mathbf{k}$ is the horizontal component of the wave vector, and $T_s \gg \omega^{-1}$. Under these conditions we can set approximately $T_s = \infty$ and integrate over the whole x, y plane. Thus we obtain

$$S_R(\mathbf{k}, \omega) = \rho^2 \alpha^2 \frac{T^2}{c_p^2} \frac{1}{L_s} \int_{R_z - L_s/2}^{R_z + L_s/2} dz_1 \int_{R_z - L_s/2}^{R_z + L_s/2} dz_2 \times e^{-ik_z(z_1 - z_2)} \tilde{S}(k_{\|}, z_1, z_2; \omega) + \text{c.c.} \tag{7.4}$$

where L_s is the height of the scattering volume, c.c. denotes the complex conjugate, and $\tilde{S}(k_{\|}, z_1, z_2; \omega)$ is defined by

$$\tilde{S}(k_{\|}, z_1, z_2; \omega) = \int_0^\infty dt \int \mathrm{d}\mathbf{r}_{\|} \, e^{-i(\mathbf{k}_{\|} \cdot \mathbf{r}_{\|} - \omega t)} S(r_{\|}, z_1, z_2; t) \tag{7.5}$$

where the $\mathbf{r}_{\|}$ integration is over the whole x, y plane.

Also of interest is the total intensity

$$I(\mathbf{k}) = \frac{1}{2\pi} \int_{-\infty}^{\infty} S(\mathbf{k}, \omega) \, d\omega \tag{7.6}$$

since it measures the density–density correlation function at equal times. Inserting, namely, (7.4), (7.5) into (7.6) one finds for the total intensity of the Rayleigh line:

$$I_R(\mathbf{k}) = \rho^2 \alpha^2 \frac{T^2}{c_p^2} \frac{1}{L_s} \int_{R_z - L_s/2}^{R_z + L_s/2} dz_1 \int_{R_z - L_s/2}^{R_z + L_s/2} dz_2 \times e^{-ik_z(z_1 - z_2)} \int d\mathbf{r}_{\|} \, e^{-i\mathbf{k}_{\|} \cdot \mathbf{r}_{\|}} S(r_{\|}, z_1, z_2; 0) \tag{7.7}$$

In the following we will discuss the expressions for the shape and the intensity of the Rayleigh line for a few cases as obtained from Eqs. (7.4), (7.5), and (7.7) by using the results for $S(r_{\|}, z_1, z_2; t)$ derived in the preceding sections of this paper.

(1) If the scattering volume is placed well inside the bulk fluid, away from the boundaries, and if the wave vector k is such that $k \gg \lambda^{-1}$, where λ is the characteristic length defined in (3.11), we may use the formula (3.8) for $S(r_\parallel, z_1, z_2; t)$, with s_+ and s_- given by (3.12). Assuming furthermore that $L_s \gg k_z^{-1}$, one can replace the bounds of the integrals over z_1 and z_2 in Eq. (7.4) by $\pm\infty$. Then one finds

$$S_R(\mathbf{k}, \omega) = k_B \rho^2 T \chi_T \frac{\gamma - 1}{\gamma} \frac{2 D_T k^2}{D_T^2 k^4 + \omega^2}$$
$$+ k_B \rho T \left(\alpha \frac{dT}{dz}\right)^2 \frac{2\nu}{\nu^2 - D_T^2} \left(\frac{1}{D_T^2 k^4 + \omega^2} - \frac{1}{\nu^2 k^4 + \omega^2}\right) \frac{k_\parallel^2}{k^4} \tag{7.8}$$

The two terms in (7.8) arise from the local equilibrium part and the mode-coupling part of $S(r_\parallel, z_1, z_2; t)$, respectively. The local equilibrium part is a Lorentzian line, centered at $\omega = 0$, with half-width $D_T k^2$. It is just the local form of the central line from the Landau–Placzek formula.[3] The mode-coupling term is not Lorentzian and anisotropic in k space. It is of second order in dT/dz and independent of the gravity field, owing to the fact that the spatial distances, probed by the wave vectors considered here, are much smaller than the characteristic length λ. The total intensity is

$$I_R(\mathbf{k}) = k_B \rho^2 T \chi_T \frac{\gamma - 1}{\gamma} + k_B \rho T \left(\alpha \frac{dT}{dz}\right)^2 \frac{1}{D_T(\nu + D_T)} \frac{\hat{k}_\parallel^2}{k^4} \tag{7.9}$$

where we have set $\hat{\mathbf{k}}_\parallel = \mathbf{k}_\parallel / k$. It follows from (7.9) that the local equilibrium part of $I_R(\mathbf{k})$ is independent of $\mathbf{k}$. This is so because the equal-time correlation matrix in equilibrium is short range,[1] so that only white noise can be detected by wave vectors from the hydrodynamic regime. The mode-coupling part, on the other hand, is proportional to k^{-4} reflecting the long-range nature of the nonequilibrium contribution to the equal-time correlation matrix [cf. Eq. (3.13a)]. The results (7.8) and (7.9) have already been derived in Ref. 6 and, for the special case $k_z = 0$, in Ref. 7 by methods different from ours. We remark that the mode-coupling correction to the Landau–Placzek expression should be observable for the wave vectors used in normal light-scattering experiments.[14]

[14] Inserting the parameters for water under normal conditions[12] and setting $dT/dz = 50\ \mathrm{K\ cm^{-1}}$, $\hat{k}_\parallel = 1$, one finds for the ratio of the mode-coupling to the local-equilibrium contribution to the Rayleigh line

$$\frac{S_R^{\mathrm{M.C.}}(\mathbf{k}, 0)}{S_R^{\mathrm{L.E.}}(\mathbf{k}, 0)} = \frac{(\alpha\, dT/dz)^2 \hat{k}_\parallel^2}{\rho \chi_T [(\gamma - 1)/\gamma]\, \nu D_T} \frac{1}{k^4} = \frac{\nu}{\nu + D_T} \frac{I_R^{\mathrm{H.C.}}(\mathbf{k})}{I_R^{\mathrm{L.E.}}(\mathbf{k})} \approx 2.5 \times 10^{13}\ \mathrm{cm^{-4}} \times \frac{1}{k^4}$$
$$\approx \begin{array}{ll} 0.3 & k = 3000\ \mathrm{cm^{-1}} \\ 1.6 & \text{for } k = 2000\ \mathrm{cm^{-1}} \\ 25 & k = 1000\ \mathrm{cm^{-1}} \end{array}$$

(2) Using very small wave vectors, i.e., $k \lesssim \lambda^{-1}$, one can probe correlations between points with distances so large that gravity and possibly boundary effects can no longer be neglected. In this regime, the mode-coupling contribution to the structure factor $S_R(\mathbf{k}, \omega)$ is many orders of magnitude larger than the local equilibrium contribution.[15] As in Sections 4–6 we will restrict ourselves here to systems for which $d \approx l_0 \ll L_\nabla$. Furthermore we choose $R_z = 0$ and $L_s = d$ so that the whole layer is illuminated by the light beam. Inserting then Eqs. (2.8)–(2.10) into (7.4), (7.5) and expressing the result in terms of the dimensionless quantities given by (4.10), we find after a straightforward calculation

$$S_R(\mathbf{k}, \omega) = 2k_B \frac{\nu}{d^2} \frac{\rho T}{g^2} \sum_n \frac{\mathscr{F}_n}{\sigma_n - i\bar{\omega}} + \text{c.c.} \tag{7.10}$$

where we have introduced the scaled frequency

$$\bar{\omega} = \frac{d^2}{\nu} \omega \tag{7.11}$$

and the oscillator strengths $\mathscr{F}_n$ defined by

$$\mathscr{F}_n(k_z; a, R) = \frac{1}{a^4} \tilde{\Theta}_n(k_z) \sum_m \frac{\Upsilon_{nm}}{\sigma_n + \sigma_m} \tilde{\Theta}_m(-k_z) \tag{7.12}$$

with

$$\Upsilon_{nm} = \frac{1}{2a^2} \int_{-1/2}^{1/2} [\Theta_n W_m + W_n \Theta_m] \, d\zeta \tag{7.13}$$

and

$$\tilde{\Theta}_n(k_z) = \int_{-1/2}^{1/2} e^{-ik_z d\zeta} \Theta_n(\zeta) \, d\zeta \tag{7.14}$$

In (7.12) we have neglected the local equilibrium contribution. Inserting (7.10) into (7.6) one finds for the total intensity

$$I_R(\mathbf{k}) = k_B \frac{\nu^2}{d^4} \frac{\rho T}{g^2} \sum_n \mathscr{F}_n + \text{c.c.} \tag{7.15}$$

[15] Since the eigenvalues s_+ and s_-, defined in (3.5), are still of the order νk^2, $D_T k^2$ when k decreases, we may use the ratio from the previous footnote, which was based on (7.8), for a rough estimate. Putting as a typical value $k = 30\,\text{cm}^{-1}$ (recall that $\lambda = 0.03$ according to footnote 5) one obtains

$$\frac{S_R^{\text{M.C.}}(\mathbf{k}, 0)}{S_R^{\text{L.E.}}(\mathbf{k}, 0)} \approx 3 \times 10^7$$

For later use we introduce also the normalized structure factor

$$\bar{S}_R(\mathbf{k}, \bar{\omega}) = \frac{\nu}{d^2} \frac{S_R(\mathbf{k}, \omega)}{I_R(\mathbf{k})} \tag{7.16}$$

which will be plotted in Figs. 3 and 4 below. With (7.10) and (7.15) we find

$$\bar{S}_R(\mathbf{k}, \bar{\omega}) = \frac{2}{\sum_n \mathrm{Re}\, \mathscr{F}_n} \sum_n \frac{(\mathrm{Re}\, \mathscr{F}_n)(\mathrm{Re}\, \sigma_n) - (\mathrm{Im}\, \mathscr{F}_n)(\bar{\omega} - \mathrm{Im}\, \sigma_n)}{(\mathrm{Re}\, \sigma_n)^2 + (\omega - \mathrm{Im}\, \sigma_n)^2} \tag{7.17}$$

(3) At the convective instability ($R = R_c$) and for a wave vector $\mathbf{k}$, the horizontal component of which has the critical magnitude $k_{\|c} = a_c/d$, the structure factor (7.10) diverges for all ω ("critical" opalescence). The reason for this singularity is the divergence at $a = a_c$ and $R = R_c$ of the oscillator strength $\mathscr{F}^{(1)}$ corresponding to the critical mode $\sigma^{(1)}(a, R)$. Near the instability point one has according to (6.3) and (6.7)

$$\sigma^{(1)}(a, R) \approx \Gamma_P \frac{\Lambda^2}{a_c^2} [(a - a_c)^2 + \varepsilon^2] \qquad (\varepsilon \to 0, a \approx a_c) \tag{7.18}$$

so that

$$\mathscr{F}^{(1)} = \frac{1}{2} K_P \frac{1}{(a - a_c)^2 + \varepsilon^2} \tilde{\Theta}_c(k_z)\, \tilde{\Theta}_c(-k_z) \qquad (\varepsilon \to 0, a \approx a_c) \tag{7.19}$$

where also (6.9) and (6.12) have been used and where

$$\tilde{\Theta}_c(k_z) = \int_{-1/2}^{1/2} e^{-ik_z d\zeta} \Theta_c(\zeta) \tag{7.20}$$

The explicit expression for the function $\tilde{\Theta}_c(k_z)$ is lengthy, but can straightforwardly be evaluated from the results given in (6.21) for stick boundary conditions. From (7.10) follows that near the instability point the dynamic structure factor has the form of a simple Lorentzian peak

$$S_R(\mathbf{k}, \omega) \approx 2k_B \frac{\nu}{d^2} \frac{\rho T}{g^2} \mathscr{F}^{(1)} \frac{2\sigma^{(1)}}{(\sigma^{(1)})^2 + \bar{\omega}^2} \qquad (R \to R_c, a \approx a_c) \tag{7.21}$$

with a linewidth going to zero like $\sigma^{(1)}$ and with a height going to infinity proportional to $1/(\sigma^{(1)})^2$.[22]

(4) We have also computed the normalized structure factors $\bar{S}_R(\mathbf{k}, \bar{\omega})$ in two stationary states away from the instability, characterized by the Rayleigh numbers $R = 1000$ (heating from below) and $R = -10\,000$ (heating from above), respectively. In our examples we have chosen the

822/40/3-4-7

Table II. Numerical Values for the Eigenvalues and Oscillator Strengths used in the Calculation of the Dynamic Structure Factor for Stick Boundary Conditions

	$R = 1000$			$R = -10000$		
		$\mathscr{F}_n$			$\mathscr{F}_n$	
n	σ_n	$k_z = 0$	$k_z = \pi/d$	σ_n	$k_z = 0$	$k_z = \pi/d$
1	4.14	3507	2341	$26.5 + 38.0i$	$13580 + 9850i$	$9470 + 6670i$
2	15.6	0	16.4	$26.5 - 38.0i$	$13580 - 9850i$	$9470 - 6670i$
3	30.0	−82.0	1.0	30.3	0	18500
4	48.0	−735	−162	35.0	1760	93
5	49.4	0	−25.0	51.5	0	1210
6	74.2	−23.7	0.25	75.2	17	40
7	92.7	0	−145	78.0	0	5364

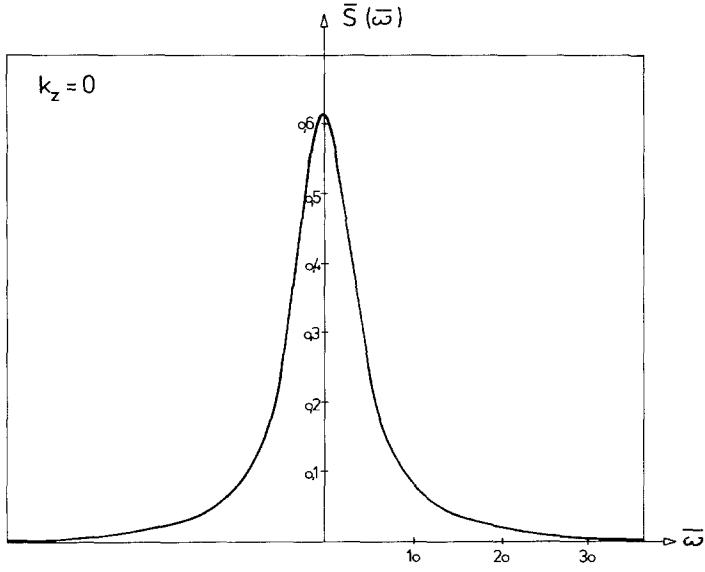

(a)

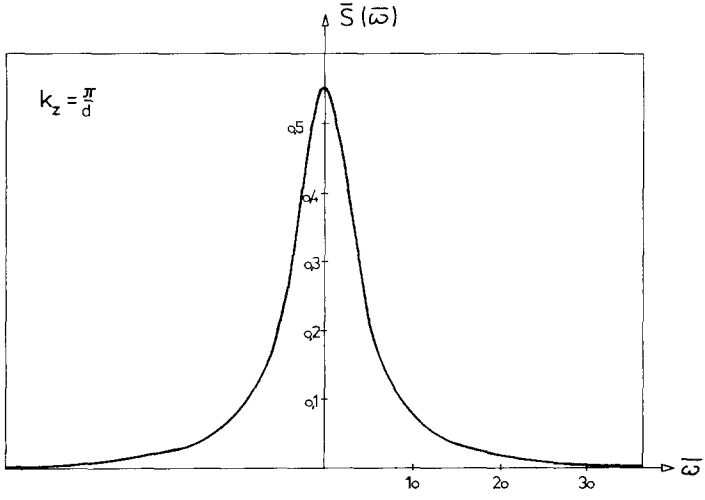

(b)

Fig. 3. Normalized dynamic structure factor $\bar{S}(\bar{\omega})$ for $P = 3.6$, $a = 4.5553$ and $R = +1000$. The vertical wave numbers are as follows: Fig. 3a, $k_z = 0$; Fig. 3b, $k_z = \pi/d$.

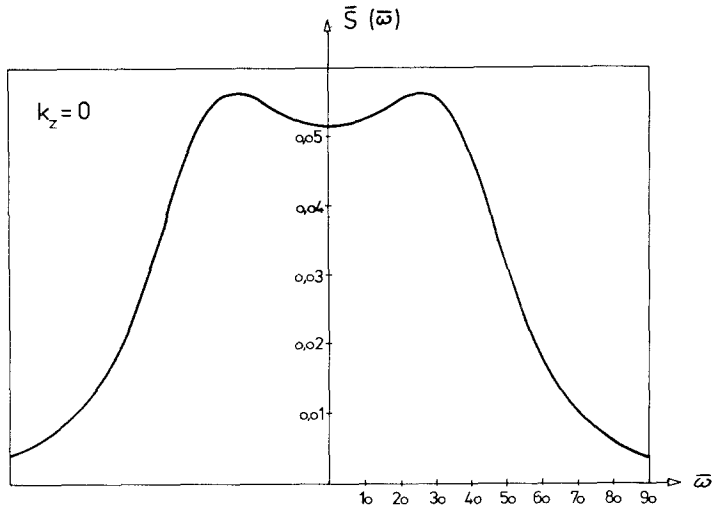

(a)

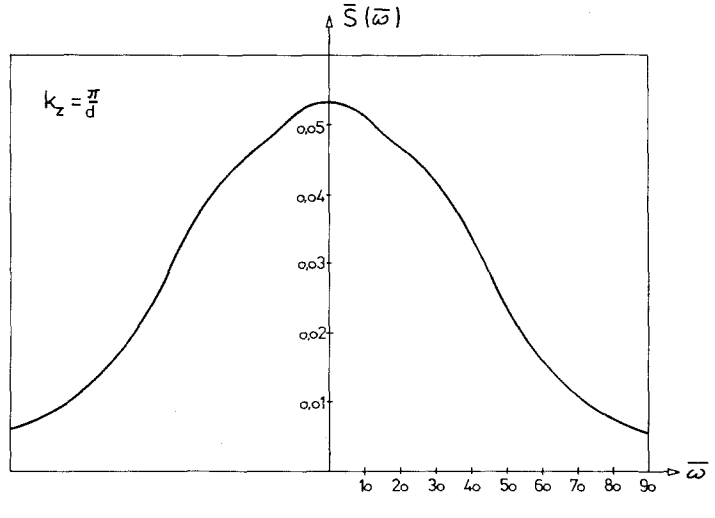

(b)

Fig. 4. Normalized dynamic structure factor $\bar{S}(\bar{\omega})$ for $P = 3.6$, $a = 4.5553$ and $R = -10\,000$. The vertical wave numbers are as follows: Fig. 4a, $k_z = 0$; Fig. 4b, $k_z = \pi/d$. Notice the different scales in Figs. 3 and 4.

Prandtl number $P = 3.6$ and the horizontal wave number $a = 4.5553$, in agreement with the choice made by Allain *et al.*[17,15] in their experiments on the propagation of the visco-heat modes. We have performed the calculations for $k_z = 0$ and for $k_z = \pi/d$. In Table II we give the numerical results for the eigenvalues σ_n of the modes we have taken into account in the sum (7.12) and the resulting oscillator strengths $\mathscr{F}_n$.

Figures 3a and 3b show $\bar{S}_R(\mathbf{k}, \omega)$ as function of $\bar{\omega}$ for $R = 1000$ and for $k_z = 0$ and $k_z = \pi/d$, respectively. As follows from Table II, the line shape is dominated in both cases by the mode $n = 1$, so that the lines have approximately a Lorentzian shape with half-width $\sigma_1 = 4.14$. On the other hand, the graphs for $R = -10\,000$, shown in Figs. 4a and 4b, are much broader. In the case $k_z = 0$ one can easily distinguish two peaks that are symmetrically shifted away from $\bar{\omega} = 0$. This kind of "second sound" phenomenon[23] is caused by the modes $n = 1$ and $n = 2$ which propagate for $R = -10\,000$ (see Table II). For $k_z = \pi/d$ this effect is obscured, however, owing to the large contribution of the next mode, i.e., $n = 3$, which does not propagate.

8. DISCUSSION

(1) Measurements of the light-scattering spectrum for small wave vectors $\mathbf{k}$ require small scattering angles due to the Bragg condition.[2] In praxis, there is a lower bound on $\mathbf{k}$, depending on the smallest angle, for which one is able to separate the scattered beam from the incident beam, and on the wavelength of the incident beam. Using a laser beam with a frequency in the range of normal light, i.e., $\omega_i \approx 3 \times 10^{15}\ \text{sec}^{-1}$, one needs a scattering angle of the order $1°$ to measure $S_R(\mathbf{k}, \omega)$ for $k \approx 2000\ \text{cm}^{-1}$, which is a typical wavevector for which Eq. (7.8), i.e., the mode-coupling correction to the local equilibrium result, could be verified (cf. Footnote 14). On the other hand, the results plotted in Figs. 3 and 4 hold for k of the order $30\ \text{cm}^{-1}$. In order to verify these results experimentally, a reduction of the wavelength of the incident beam to the infrared or microwave regime seems to be necessary. Unfortunately most molecular substances absorb these frequencies. Nevertheless there may be fluids from which microwaves are scattered. Perhaps a heavy inert gas, like xenon, could be a candidate.

(2) As has been pointed out in Section 5, the existence of propagating visco-heat modes has been established experimentally by Allain *et al.*[17] However, these experiments have been performed only for Rayleigh numbers far beyond the threshold of propagation of the particular mode that was excited, i.e., far beyond its branch point. When the squares of the measured frequencies of the waves (i.e., the imaginary parts

of the eigenvalues) are plotted against the Rayleigh number, they seem to lie on a straight line, as predicted by the parabolic approximation (5.1). For suitably chosen conditions on the horizontal wave number, more careful measurements should yield large deviations from the straight line near the propagation threshold, confirming the shift of the branch point from the value predicted by the parabolic approximation, owing to the avoidance of crossing. Moreover, the slope in the threshold would determine the coefficient α_1 in Eq. (5.2). Finally, the experimental observation of a "window of propagation" would be of special interest. Experiments near the threshold or within the "windows" are very difficult, however, since here the propagation is very small compared to the damping.

(3) As already discussed in Refs. 9 and 10, the results for the singular behavior of the correlation matrix near the instability, presented in Section 6, cannot be applied to the immediate vicinity of R_c. The reason for the failure of the theory is that the magnitude of the fluctuations becomes larger and larger as $R \to R_c$, and hence the linear fluctuation theory, used in this paper, breaks down. To use the language of critical phenomena, our theory is just a mean field theory. Attempts to go beyond a mean field theory, by taking into account the fluctuations in a nonlinear way[24] or using renormalized transport coefficients,[10] indicate that the region, where the mean field theory breaks down, is unaccessible close to R_c, at least with the present experimental possibilities.

(4) For wave vectors in the regime probed by normal light-scattering ($k \approx 2000\ \text{cm}^{-1}$), van der Zwan *et al.*[25] have also computed the dynamic structure factor of the Rayleigh line. They use a perturbation theory around equilibrium in the temperature gradient, taking explicitly into account the variation of the average quantities with position. This yields a line shape that is not symmetric in ω. However, as the authors point out, this effect is unobservably small. To understand this better, we recall from I that for the slow modes the variation of the average quantities with position can be neglected for all wave vectors with $k_z \gtrsim l_0^{-1}$. Clearly, it can therefore also be neglected in normal light scattering, where even $k_z \gg l_0^{-1}$.

(5) In the problems discussed in this paper, the condition $k_z \gtrsim l_0^{-1}$ was always satisfied, and the Boussinesq equations, derived in I, were sufficient for us to determine the slow modes. Nevertheless, there are situations where the spatial variation of the average quantities has to be taken into account explicitly, even for the slow modes. They occur in systems where $d \approx L_\nabla \gg l_0$, so that modes with very long "wavelengths" (i.e., of the order L_∇) are possible. In order to compute these modes, one has first to extend the Boussinesq equations. Deriving the correct extension of the Boussinesq equations from the full linearized hydrodynamic equations should be feasible with the methods developed in paper I. An interesting

application of these extended Boussinesq equations would be the calculation of the instability point in a Rayleigh–Bénard system where d can be of the same order as L_∇. This would lead to a value of R_c different from $R_c = 1707.762$, which is only valid for $d \ll L_\nabla$.

ACKNOWLEDGMENTS

The authors wish to thank Dr. M. López de Haro and Dr. T. B. Ong for their assistance in the numerical computations. This work was in part performed under National Science Foundation Contract No. MCS 80-17781 and DOE Contract No. DE-ACO2-ER10807.006.

APPENDIX A

In this appendix we derive the left eigenvalue equations for the visco-heat modes. To this purpose we consider the space of all vectors

$$\mathbf{U} = \begin{pmatrix} T(z) \\ v(z) \end{pmatrix} \tag{A1}$$

where $T(z)$ and $v(z)$ are suitably often differentiable functions which satisfy the boundary conditions

$$\begin{gathered} T = 0 \\ v = 0, \quad \frac{dv}{dz} = 0 \qquad (z = \pm d/2) \end{gathered} \tag{A2}$$

$T(z)$ and $v(z)$ can be interpreted as the temperature and the z component of the transversal velocity field, respectively, of an arbitrary perturbation around the stationary state. Equations (A2) are then the boundary conditions used in the main text [cf. Eq. (4.11)].

Defining the operators

$$\mathscr{L} = \begin{pmatrix} D_T \mathscr{D} & \dfrac{dT}{dz} \\ -\alpha g k_\parallel^2 & \nu \mathscr{D}^2 \end{pmatrix} \tag{A3}$$

with $\mathscr{D} = k_\parallel^2 - d^2/dz^2$ and

$$\mathsf{D} = \begin{pmatrix} 1 & 0 \\ 0 & \mathscr{D} \end{pmatrix} \tag{A4}$$

we can write the right eigenvalue equations (2.6) in the form

$$\mathscr{L} \cdot \mathbf{U}_n^R = s_n \mathsf{D} \cdot \mathbf{U}_n^R \tag{A5}$$

Furthermore we write the normalization condition (2.7) as

$$(\mathsf{K} \cdot \mathbf{U}_m^L, \mathsf{D} \cdot \mathbf{U}_n^R) = \frac{k_\parallel^2}{(2\pi)^2} \delta_{nm} \tag{A6}$$

where we have set

$$\mathsf{K} = \begin{pmatrix} k_\parallel^2 & 0 \\ 0 & 1 \end{pmatrix} \tag{A7}$$

and introduced the scalar product

$$(\mathbf{U}_1, \mathbf{U}_2) = \int_{-d/2}^{d/2} [T_1^* T_2 + v_1^* v_2] \, dz \tag{A8}$$

for arbitrary vectors $\mathbf{U}_1$ and $\mathbf{U}_2$.

Multiplying (A6) by the eigenvalue s_n yields

$$\begin{aligned} s_n \frac{k_\parallel^2}{(2\pi)^2} \delta_{nm} &= (\mathsf{K} \cdot \mathbf{U}_m^L, s_n \mathsf{D} \cdot \mathbf{U}_n^R) = (\mathsf{K} \cdot \mathbf{U}_m^L, \mathscr{L} \cdot \mathbf{U}_n^R) \\ &= s_m \frac{k_\parallel^2}{(2\pi)^2} \delta_{nm} = (s_m^* \mathsf{D} \cdot \mathbf{U}_m^L, \mathsf{K} \cdot \mathbf{U}_n^R) \end{aligned} \tag{A9}$$

where we have used the boundary conditions and that K and D commute. Hence, the left eigenvalue equation is

$$\mathscr{L}^\dagger \cdot \mathbf{U}_m^L = s_m^* \mathsf{D} \cdot \mathbf{U}_m^L \tag{A10}$$

where the adjoint operator $\mathscr{L}^\dagger$ has to be determined from the equation

$$(\mathsf{K} \cdot \mathbf{U}_1, \mathscr{L} \cdot \mathbf{U}_2) = (\mathscr{L}^\dagger \cdot \mathbf{U}_1, \mathsf{K} \cdot \mathbf{U}_2) \tag{A11}$$

for arbitrary vectors $\mathbf{U}_1$, $\mathbf{U}_2$ satisfying the boundary conditions. Integrating the left-hand side (l.h.s.) of (A11) by parts, using (A2),[16] one obtains

$$\mathscr{L}^\dagger = \begin{pmatrix} D_T \mathscr{D} & -\alpha g \\ \dfrac{dT}{dz} k_\parallel^2 & \nu \mathscr{D}^2 \end{pmatrix} \tag{A12}$$

[16] We require that the left eigenvectors obey the same boundary conditions as the right eigenvectors.

Hence the left eigenvalue equations (A10) read explicitly

$$\begin{pmatrix} D_T\mathscr{D} & -\alpha g \\ \dfrac{dT}{dz}k_{\|}^2 & \nu\mathscr{D}^2 \end{pmatrix} \begin{pmatrix} T^L_{\lambda,k_{\|}n}(z) \\ v^L_{\lambda,k_{\|}n}(z) \end{pmatrix} = s^*_{\lambda,k_{\|}n} \begin{pmatrix} T^L_{\lambda,k_{\|}n}(z) \\ \mathscr{D}v^L_{\lambda,k_{\|}n}(z) \end{pmatrix} \tag{A13}$$

We remark finally that (A13) is still correct when the stick boundary condition $dv/dz = 0$ $(z = \pm d/2)$ in (A2) is replaced by the slip condition $d^2v/dz^2 = 0$ $(z = \pm d/2)$.

APPENDIX B

In this appendix we show first that the components $T^L_{\lambda,k_{\|}n}(z)$ and $v^L_{\lambda,k_{\|}n}(z)$ of the left eigenvectors of the visco-heat modes are proportional to $\Theta^*_n(\zeta)$ and $W^*_n(\zeta)$, where $\Theta_n(\zeta)$ and $W_n(\zeta)$ are the dimensionless functions that have been introduced by (4.6) and (4.7). We have used this property in deriving Eq. (4.9). Then we will define the projection operators $\mathscr{P}_n$ corresponding to the eigenvalues σ_n, and finally we will prove two simple properties of the eigenvalues that have been used in Sections 5 and 6.

Defining the function $W^L_n(\zeta)$ by

$$v^L_{\lambda,k_{\|}n}(z) = W^L_n(\zeta) \tag{B1}$$

we obtain from the second equation in (A13),

$$T^L_{\lambda,k_{\|}n}(z) = -\frac{\nu}{d^2}\frac{1}{(dT/dz)\,a^2}\Theta^L_n(\zeta) \tag{B2}$$

where

$$\Theta^L_n(\zeta) = \left(a^2 - \frac{d^2}{d\zeta^2} - \sigma^*_n\right)\left(a^2 - \frac{d^2}{d\zeta^2}\right) W^L_n(\zeta) \tag{B3}$$

Inserting (B2) into the first equation in (A13) yields

$$\left(a^2 - \frac{d^2}{d\zeta^2} - P\sigma^*_n\right)\Theta^L_n(\zeta) = Ra^2 W^L_n(\zeta) \tag{B4}$$

The last two equations for Θ^L_n and W^L_n are identical to Eqs. (4.8), provided that σ_n is replaced by σ^*_n. Furthermore, the left eigenvectors obey the same boundary conditions as the right eigenvectors. Since the coefficients a, R, and P are real it follows that

$$\Theta^L_n = c\Theta^*_n, \qquad W^L_n = cW^*_n \tag{B5}$$

where c is an arbitrary constant. Combining (B1), (B2), and (B5) the statement made above follows.

In order to define the projection operators $\mathscr{P}_n$ we use a notation similar to that of the preceding appendix, but for the dimensionless quantities. Thus we set

$$\mathbf{U}_n = \begin{pmatrix} \Theta_n(\zeta) \\ W_n(\zeta) \end{pmatrix} \tag{B6}$$

and write the eigenvalue equations (4.8) and the normalization (4.9) as

$$\mathscr{L} \cdot \mathbf{U}_n = \sigma_n \mathsf{D} \cdot \mathbf{U}_n \tag{B7}$$

$$(\mathsf{K} \cdot \mathbf{U}_m^*, \mathsf{D} \cdot \mathbf{U}_n) = \delta_{nm} \tag{B8}$$

where now

$$\mathscr{L} = \begin{pmatrix} \frac{1}{P}\left(a^2 - \frac{d^2}{d\zeta^2}\right) & -\frac{Ra^2}{P} \\ -1 & \left(a^2 - \frac{d^2}{d\zeta^2}\right)^2 \end{pmatrix} \tag{B9}$$

and

$$\mathsf{D} = \begin{pmatrix} 1 & 0 \\ 0 & a^2 - \frac{d^2}{d\zeta^2} \end{pmatrix}, \qquad \mathsf{K} = \begin{pmatrix} \frac{P}{Ra^4} & 0 \\ 0 & \frac{1}{a^2} \end{pmatrix} \tag{B10}$$

The dimensionless operator $\mathscr{L}$ is self-adjoint in the scalar product (B8).

The eigenprojection operator $\mathscr{P}_n$ is defined by

$$\mathscr{P}_n \mathbf{U} = u_n \mathbf{U}_n \tag{B11}$$

where $\mathbf{U}$ is an arbitrary vector that can be expanded in terms of the eigenvectors $\mathbf{U}_m$ as

$$\mathbf{U} = \sum_m u_m \mathbf{U}_m \tag{B12}$$

with expansion coefficients u_m. With the aid of (B8) we obtain

$$u_n = (\mathsf{K} \cdot \mathsf{D} \cdot \mathbf{U}_n^*, \mathbf{U}) \tag{B13}$$

Inserting (B13) into (B11) yields

$$(\mathscr{P}_n \mathbf{U})(\zeta) = \int \mathsf{P}_n(\zeta, \zeta') \cdot \mathbf{U}(\zeta') \tag{B14}$$

where the integral kernel $\mathsf{P}_n(\zeta, \zeta')$ is defined as the dyadic

$$\mathsf{P}_n(\zeta, \zeta') = \mathbf{U}_n(\zeta)\mathsf{K} \cdot \mathsf{D} \cdot \mathbf{U}_n^*(\zeta') \tag{B15}$$

Inserting (B6) and (B10) into (B15) we find explicitly

$$\mathsf{P}_n(\zeta, \zeta') = \begin{pmatrix} \dfrac{P}{Ra^4}\Theta_n(\zeta)\,\Theta_n^*(\zeta') & \dfrac{1}{a^2}\Theta_n(\zeta)\left(a^2 - \dfrac{d^2}{d\zeta'^2}\right) W_n^*(\zeta') \\ \dfrac{P}{Ra^4} W_n(\zeta)\,\Theta_n^*(\zeta') & \dfrac{1}{a^2} W_n(\zeta)\left(a^2 - \dfrac{d^2}{d\zeta'^2}\right) W_n^*(\zeta') \end{pmatrix} \tag{B16}$$

Finally we prove two simple properties of the eigenvalues σ_n used in Sections 5 and 6. Following Ref. 14 we write (4.8) in the form

$$\begin{aligned} \sigma_n\left(a^2 - \frac{d^2}{d\zeta^2}\right) W_n &= -\Theta_n + \left(a^2 - \frac{d^2}{d\zeta^2}\right)^2 W_n \\ P\sigma_n \Theta_n &= -Ra^2 W_n + \left(a^2 - \frac{d^2}{d\zeta^2}\right)\Theta_n \end{aligned} \tag{B17}$$

Multiplying the first equation by W_n^* and the second equation by Θ_n^* and integrating over ζ from $-1/2$ to $+1/2$ yields

$$\begin{aligned} &\sigma_n \int_{-1/2}^{1/2} W_n^*\left(a^2 - \frac{d^2}{d\zeta^2}\right) W_n \, d\zeta \\ &\quad = -\int_{-1/2}^{1/2} W_n^* \Theta_n \, d\zeta + \int_{-1/2}^{1/2} W_n^*\left(a^2 - \frac{d^2}{d\zeta^2}\right)^2 W_n \, d\zeta \\ &P\sigma_n \int_{-1/2}^{1/2} \Theta_n^* \Theta_n \, d\zeta \\ &\quad = -Ra^2 \int_{-1/2}^{1/2} \Theta_n^* W_n \, d\zeta + \int_{-1/2}^{1/2} \Theta_n^*\left(a^2 - \frac{d^2}{d\zeta^2}\right)\Theta_n \, d\zeta \end{aligned} \tag{B18}$$

Now take the complex conjugate equations of (B18) and subtract them from (B18). This yields

$$\begin{aligned} (\sigma_n - \sigma_n^*) \int_{-1/2}^{1/2} W_n^*\left(a^2 - \frac{d^2}{d\zeta^2}\right) W_n \, d\zeta &= -\int_{-1/2}^{1/2} (W_n^* \Theta_n - W_n \Theta_n^*) \, d\zeta \\ P(\sigma_n - \sigma_n^*) \int_{-1/2}^{1/2} \Theta_n^* \Theta_n \, d\zeta &= -Ra^2 \int_{-1/2}^{1/2} (\Theta_n^* W_n - \Theta_n W_n^*) \, d\zeta \end{aligned} \tag{B19}$$

where also the boundary conditions have been used during partial integration. Eliminating the r.h.s. between Eqs. (B19) one finds

$$(\sigma_n - \sigma_n^*) \int_{-1/2}^{1/2} \left[|W_n|^2 + \frac{1}{a^2} \left| \frac{dW_n}{d\zeta} \right|^2 + \frac{P}{Ra^4} |\Theta_n|^2 \right] d\zeta = 0 \qquad \text{(B20)}$$

Since the integral is positive for all $R > 0$ it follows from (B20) that $\sigma_n = \sigma_n^*$ for $R > 0$. In other words, the eigenvalues are real if the system is heated from below, or, propagation can only occur when the fluid is heated from above.

Similarly, one can take the complex conjugate equations of (B18) and add them to (B18). Then one finds

$$\begin{aligned}
&(\sigma_n + \sigma_n^*) \int_{-1/2}^{1/2} W_n^* \left(a^2 - \frac{d^2}{d\zeta^2} \right) W_n \, d\zeta \\
&\quad = -\int_{-1/2}^{1/2} (W_n^* \Theta_n + \Theta_n^* W_n) \, d\zeta + 2 \int_{-1/2}^{1/2} W_n^* \left(a^2 - \frac{d^2}{d\zeta^2} \right)^2 W_n \, d\zeta \\
&P(\sigma_n + \sigma_n^*) \int_{-1/2}^{1/2} \Theta_n^* \Theta_n \, d\zeta \\
&\quad = -Ra^2 \int_{-1/2}^{1/2} (\Theta_n^* W_n + W_n^* \Theta_n) \, d\zeta + 2 \int_{-1/2}^{1/2} \Theta_n^* \left(a^2 - \frac{d^2}{d\zeta^2} \right) \Theta_n \, d\zeta
\end{aligned} \qquad \text{(B21)}$$

Multiplying the first equation of (B21) by Ra^2 and subtracting it from the second one finds finally

$$\begin{aligned}
&(\sigma_n + \sigma_n^*) \int_{-1/2}^{1/2} \left[|W_n|^2 + \frac{1}{a^2} \left| \frac{dW_n}{d\zeta} \right|^2 - \frac{P}{Ra^4} |\Theta_n|^2 \right] d\zeta \\
&\quad = 2 \int_{-1/2}^{1/2} \left[\frac{1}{a^2} \left| \left(a^2 - \frac{d^2}{d\zeta^2} \right) W_n \right|^2 - \frac{1}{Ra^2} \left(|\Theta_n|^2 + \frac{1}{a^2} \left| \frac{d\Theta_n}{d\zeta} \right|^2 \right) \right] d\zeta
\end{aligned} \qquad \text{(B22)}$$

The integrals in (B22) are both positive if $R < 0$. Hence it follows that $\sigma_n + \sigma_n^* > 0$ for $R < 0$. In other words, the real part of σ_n is positive if the system is heated from above, or, the system can become unstable, only when it is heated from below.

APPENDIX C

In this appendix we give expressions for the quantities σ_{nH}, σ_{nv}, and R_{nC} that are used in the parabolic approximation (5.1). σ_{nH} and σ_{nv} are defined to be the solutions of the characteristic equations $F^E(\sigma; a, R) = 0$

and $F^0(\sigma; a, R) = 0$, respectively, for $R = 0$. To compute σ_{nH} and σ_{nv} observe first that the three roots of (4.14) in the right half of the complex plane are $q_1(\sigma) = ia$, $q_2(\sigma) = (\sigma - a^2)^{1/2}$ and $q_3(\sigma) = (P\sigma - a^2)^{1/2}$. Since $Q_1 = 0$ and $Q_2 = \sigma$ it follows that the characteristic functions $F^E(\sigma; a, 0)$ and $F^0(\sigma; a, 0)$, respectively, factorize, e.g.,

$$\begin{aligned} &F^E(\sigma; a, 0) \\ &\quad = \left[P(P-1)\sigma \cos\frac{q_3}{2} \right] \cdot \left[q_2 \cos\frac{q_1}{2} \sin\frac{q_2}{2} - q_1 \sin\frac{q_1}{2} \cos\frac{q_2}{2} \right] \\ &\quad = F_H^E(\sigma; a) \cdot F_v^E(\sigma; a) \end{aligned} \tag{C1}$$

Setting $F_H^E(\sigma; a)$ and $F_H^0(\sigma; a)$ equal to zero yields $q_{n3} = n\pi$ $(n = 1, 2, 3, \ldots)$. This leads to the eigenvalues

$$\sigma_{nH}(a) = \frac{1}{P}(a^2 + n^2\pi^2) \qquad (n = 1, 2, 3, \ldots) \tag{C2}$$

Setting $F_v^E(\sigma; a)$ and $F_v^0(\sigma; a)$ equal to zero yields $q_{n2} = b_n$ $(n = 1, 2, 3, \ldots)$ where b_n is the nth positive solution of

$$\begin{aligned} b \tan\frac{b}{2} + a \tanh\frac{a}{2} &= 0 \qquad (n = 1, 3, \ldots) \\ b \cot\frac{b}{2} - a \coth\frac{a}{2} &= 0 \qquad (n = 2, 4, \ldots) \end{aligned} \tag{C3}$$

The corresponding eigenvalues are

$$\sigma_{nv}(a) = a^2 + b_n^2 \qquad (n, 1, 2, 3, \ldots) \tag{C4}$$

Looking at the normalized eigenfunctions (4.10) in the limit $dT/dz \to 0$ it is easy to identify σ_{nH} and σ_{nv} as the eigenvalues of the heat and viscous modes, respectively, in equilibrium for stick boundary conditions.

To determine $R_{nC}(a)$ exactly one can set $\sigma = 0$ in Eqs. (4.14)–(4.16) and solve the characteristic equations $F^E(0; a, R) = 0$ and $F^0(0; a, R) = 0$ numerically for R. Alternatively one can use an approximate expression for $R_{nC}(a)$ that has been derived by Chandrasekhar[11] using a variational principle:

$$R_{nC}(a) \approx \frac{(n^2\pi^2 + a^2)^3}{a^2} \left[1 - 16 \frac{n^2\pi^2}{(n^2\pi^2 + a^2)^2} \rho_n(a) \right]^{-1} \tag{C5}$$

where

$$\rho_n(a) = \begin{cases} \dfrac{a\cosh^2(a/2)}{\sinh a + a} & (n = 1, 3, \ldots) \\ \dfrac{a\sinh^2 a}{\sinh a - a} & (n = 2, 4, \ldots) \end{cases} \tag{C6}$$

The accuracy of (C5) is around 1% or better for low n and the values of a in the range $1 \leqslant a \leqslant 10$ that have been used in Fig. 1.

APPENDIX D

In the last appendix we illustrate the formal expansions (5.2) and (5.3), which have been proven by Kato,[18] by deriving explicit expressions for the eigenvalues σ_n and the eigenprojections $\mathscr{P}_n$ near a branch point for slip boundary conditions. For slip boundary conditions the eigenvalues of (4.8) are simply[8]

$$\sigma_{n\pm}(R) = \frac{P+1}{2P}(a^2 + n^2\pi^2) \pm \frac{P-1}{2P}(a^2 + n^2\pi^2) \times \left[1 + \frac{4P}{(P-1)^2}\frac{Ra^2}{(a^2 + n^2\pi^2)^3}\right]^{1/2} \tag{D1}$$

while the components of the eigenvectors are

$$\begin{aligned} \Theta_{n\pm}(\zeta) &= N_{n\pm}(a^2 + n^2\pi^2 - \sigma_{n\pm})(a^2 + n^2\pi^2)\, I_n(\zeta) \\ W_{n\pm}(\zeta) &= N_{n\pm}\, I_n(\zeta) \end{aligned} \tag{D2}$$

where $N_{n\pm}$ is a normalization constant and

$$I_n(\zeta) = \begin{cases} \cos n\pi\zeta & (n = 1, 3, 5, \ldots) \\ \sin n\pi\zeta & (n = 2, 4, 6, \ldots) \end{cases} \tag{D3}$$

Using the identity

$$\frac{P}{Ra^2}(a^2 + n^2\pi^2) = -\frac{1}{(a^2 + n^2\pi^2 - \sigma_{n+})(a^2 + n^2\pi^2 - \sigma_{n-})} \tag{D4}$$

which follows immediately from (D1), one finds from (4.9) for the normalization constants

$$N_{n\pm}^2 = \pm\frac{2a^2}{a^2 + n^2\pi^2}\frac{a^2 + n^2\pi^2 - \sigma_{n\mp}}{\sigma_{n+} - \sigma_{n-}} \tag{D5}$$

The modes $(n+)$ and $(n-)$ given by (D1) have a common branch point at

$$R_{n0} = \frac{(P-1)^2}{4P} \frac{(a^2+n^2\pi^2)^3}{a^2}$$
$$\sigma_{n0} = \frac{P+1}{2P}(a^2+n^2\pi^2) \tag{D6}$$

Inserting (D6) into (D1) we can rewrite the eigenvalues in the form

$$\sigma_{n\pm}(R) = \sigma_{n0} \pm \alpha_1 (R-R_{n0})^{1/2} \tag{D7}$$

where

$$\alpha_1 = \frac{a}{[P(a^2+n^2\pi^2)]^{1/2}} \tag{D8}$$

Equation (D7) has the form of a Puiseux series [cf. Eq. (5.2)] with coefficients α_j that vanish identically for $j>1$. This simplification does not occur for more general boundary conditions. However, in the general case, the eigenvalues have still the form (D7) if one is close enough to the branch point, as has been shown by Kato.

Inserting (D7) into (D5) yields

$$N_{n\pm}^2 = \pm \frac{P-1}{2P} a^2 \frac{1}{\alpha_1 (R-R_{n0})^{1/2}} + \frac{a^2}{a^2+n^2\pi^2} \tag{D9}$$

Thus, the eigenvector given by (D2) diverges like $(R-R_0)^{-1/4}$ as the branch point is approached. Inserting (D2), (D7), and (D9) into (B16), and neglecting terms of the order $(R-R_0)^{1/2}$, we obtain after a straightforward calculation for the kernel $\mathsf{P}_n(\zeta,\zeta')$ corresponding to the eigenprojection operator $\mathscr{P}_n$

$$\mathsf{P}_{n\pm}(\zeta,\zeta') = \pm (R-R_{n0})^{-1/2} \mathsf{N}_{n0}(\zeta,\zeta') + \tfrac{1}{2}\mathsf{P}_{n0}(\zeta,\zeta') + \cdots \tag{D10}$$

where

$$\mathsf{N}_{n0}(\zeta,\zeta') = \frac{P-1}{2P} \frac{a^2+n^2\pi^2}{\alpha_1} \begin{pmatrix} -1 & \frac{P-1}{2P}(a^2+n^2\pi^2)^2 \\ -\frac{2P}{P-1}\frac{1}{(a^2+n^2\pi^2)^2} & 1 \end{pmatrix}$$
$$\times I_n(\zeta) I_n(\zeta') \tag{D11}$$

and

$$\mathsf{P}_{n0}(\zeta, \zeta') = 2\begin{pmatrix} 1 & 0 \\ 0 & 1 \end{pmatrix} I_n(\zeta)\, I_n(\zeta') \tag{D12}$$

From the orthogonality property of the functions $I_n(\zeta)$ follows that P_{n0} is the total eigenprojection kernel corresponding to σ_{n0}, i.e., of the product space spanned by the eigenvectors of the modes $\sigma_{n+}(R)$ and $\sigma_{n-}(R)$ in the limit $R \to R_{n0}$. Furthermore one verifies easily from the special form of the matrix appearing in (D11), that the kernel N_{n0} is nilpotent. The results (D10)–(D12) are an example of the more general statement cited in part (ii) of Section 5.4.

Using (D7) and (D10) we show finally that the operator $\mathscr{L}$, defined in (B7), and the corresponding time-evolution operator $\mathscr{U}(\tau) = \exp(-\mathscr{L}\tau)$ ($\tau > 0$) are finite if there happens to be a branch point at the value of R considered. To this purpose we use the spectral representation of the integral kernels $\mathsf{L}(\zeta, \zeta')$ and $\mathsf{U}(\zeta, \zeta')$ corresponding to $\mathscr{L}$ and $\mathscr{U}$, i.e.,

$$\begin{aligned} \mathsf{L}(\zeta, \zeta') &= \sum_m \mathsf{L}_m(\zeta, \zeta') = \mathsf{D} \cdot \sum_m (\sigma_{m+}\, \mathsf{P}_{m+} + \sigma_{m-}\, \mathsf{P}_{m-}) \\ \mathsf{U}(\zeta, \zeta'; \tau) &= \sum_m \mathbf{U}_m(\zeta, \zeta') = \mathsf{D} \cdot \sum_m (e^{-\sigma_{m+}\tau}\mathsf{P}_{m+} + e^{-\sigma_{m-}\tau}\mathsf{P}_{m-}) \end{aligned} \tag{D13}$$

If there is a branch point at $R = R_{n0}$, we compute the nonanalytic part of L and U by setting first $R = R_{n0} \pm \varepsilon$, ε infinitesimal, using (D7) and (D10), and taking then the limit $\varepsilon \to 0$. This yields

$$\begin{aligned} \mathsf{L}(\zeta, \zeta) &= \mathsf{D} \cdot (\sigma_{n0}\mathsf{P}_{n0} + 2\alpha_1 \mathsf{N}_{n0}) + \sum_{m \neq n} \mathsf{L}_m \\ \mathsf{U}(\zeta, \zeta; \tau) &= \mathsf{D} \cdot (\mathsf{P}_{n0} - 2\alpha_1 \mathsf{N}_{n0}\tau)\, e^{-\sigma_{n0}\tau} + \sum_{m \neq n} \mathsf{U}_m \end{aligned} \tag{D14}$$

The last equation implies that in a branch point there are generalized eigenmodes that do not evolve exponentially with time τ, but like $\tau e^{-\sigma_{n0}\tau}$. This behavior is similar to the aperiodic limit case of a damped harmonic oscillator.

REFERENCES

1. R. Schmitz and E. G. D. Cohen, *J. Stat. Phys.* **39**: 285 (1985).
2. B. J. Berne and R. Pecora, *Dynamic Light Scattering*, (Wiley, New York, 1976), Chaps. 2–4.
3. L. D. Landau and E. M. Lifshitz, *Electrodynamics of Continuous Media* (Pergamon, New York, 1960), Section 94.

4. D. Ronis, I. Procaccia, and I. Oppenheim, *Phys. Rev. A* **19**:1324 (1979).
5. T. R. Kirkpatrick, E. G. D. Cohen, and J. R. Dorfman, *Phys. Rev. A* **26**:972 (1982).
6. T. R. Kirkpatrick, E. G. D. Cohen, and J. R. Dorfman, *Phys. Rev. A* **26**:995 (1982).
7. D. Ronis and I. Procaccia, *Phys. Rev. A* **26**:1812 (1982).
8. E. G. D. Cohen and R. Schmitz, in *Fundamental Problems in Statistical Mechanics VI*, E. G. D. Cohen, ed. (North-Holland, Amsterdam, 1985), p. 229.
9. V. M. Zaĭtsev and M. I. Shliomis, *Sov. Phys. JETP* **32**:866 (1971).
10. T. R. Kirkpatrick and E. G. D. Cohen, *J. Stat. Phys.* **33**:639 (1983).
11. S. Chandrasekhar, *Hydrodynamic and Hydromagnetic Stability* (Dover, New York, 1961), Chap. II.
12. D. E. Gray, ed., *American Institute of Physics Handbook* (McGraw-Hill, New York, 1963).
13. U. Geigenmüller, U. M. Titulaer, and B. U. Felderhof, *Physica* **119A**:41 (1983).
14. G. Z. Gershuni and E. M. Zhukhovitskii, *Convective Stability of Incompressible Fluids*, translated from the Russian (Israel Program for Scientific Translations, Jerusalem 1976), Chap. II.
15. P. Lallemand and C. Allain, *J. Phys. (Paris)* **41**:1 (1980).
16. R. Graham and H. Pleiner, *Phys. Fluids* **18**:130 (1975).
17. C. Allain, P. Lallemand, and J. P. Boon, in *Light Scattering in Liquids and Macromolecular Solutions*, V. Degiorgio, M. Corti, and M. Giglio, eds. (Plenum Press, New York, 1980); J. P. Boon, C. Allain, and P. Lallemand, *Phys. Rev. Lett.* **43**:199 (1979).
18. T. Kato, *Perturbation Theory for Linear Operators*, 2nd ed. (Springer, New York, 1980), Chap. II, Section 1.
19. J. Wesfreid, Y. Pomeau, M. Dubois, C. Normand, and P. Bergé, *J. Phys. Lett. (Paris)* **39**:725 (1978).
20. I. S. Gradshteyn and I. M. Ryzhik, *Table of Integrals, Series and Products*, 4th ed. (Academic Press, New York, 1980), p. 497.
21. M. Abramowitz and I. A. Stegun, *Handbook of Mathematical Functions* (Dover, New York, 1972), p. 298.
22. H. N. W. Lekkerkerker and J. P. Boon, *Phys. Rev. A* **10**:1355 (1974).
23. S. J. Putterman, *Superfluid Hydrodynamics* (North-Holland, Amsterdam, 1974), Section 7.
24. R. Graham and H. Pleiner, *Phys. Fluids* **18**:130 (1975).
25. G. van der Zwan, D. Bedeaux, and P. Mazur, *Physica* **107A**:491 (1981).